

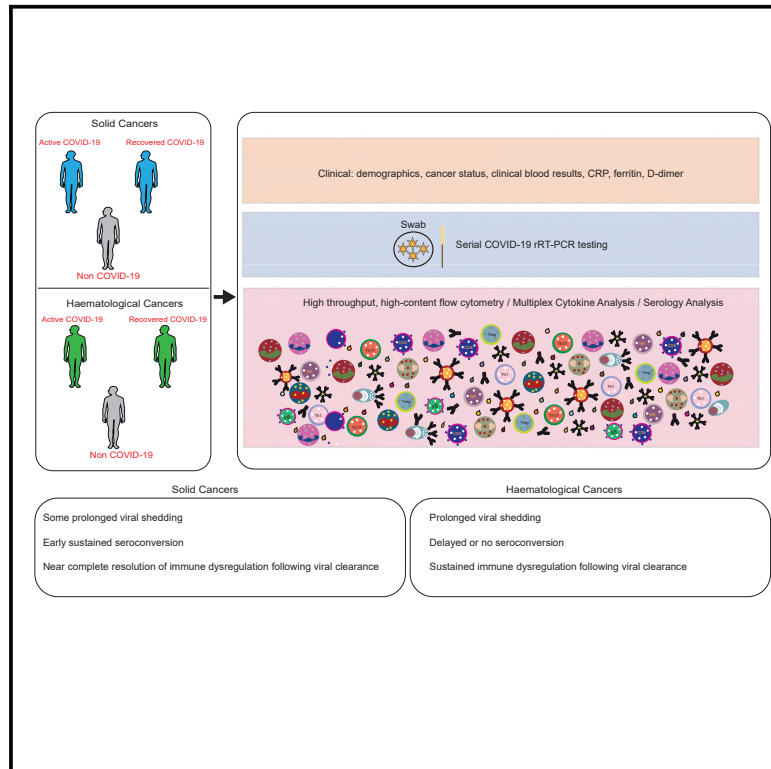


Since January 2020 Elsevier has created a COVID-19 resource centre with free information in English and Mandarin on the novel coronavirus COVID-19. The COVID-19 resource centre is hosted on Elsevier Connect, the company's public news and information website.

Elsevier hereby grants permission to make all its COVID-19-related research that is available on the COVID-19 resource centre - including this research content - immediately available in PubMed Central and other publicly funded repositories, such as the WHO COVID database with rights for unrestricted research re-use and analyses in any form or by any means with acknowledgement of the original source. These permissions are granted for free by Elsevier for as long as the COVID-19 resource centre remains active.

Acute immune signatures and their legacies in severe acute respiratory syndrome coronavirus-2 infected cancer patients

Graphical Abstract



Authors

Sultan Abdul-Jawad, Luca Baù, Thanussuyah Alaguthurai, ..., Adrian C. Hayday, Piers E.M. Patten, Sheeba Irshad

Correspondence

sheeba.irshad@kcl.ac.uk

In Brief

Following SARS-Cov-2 infection, Sultan et al. showed that the majority of solid cancer patients cleared virus, recovered from COVID-19, and re-established their prior immunological status. In contrast, hematological cancer patients demonstrated delayed or negligible seroconversion, prolonged shedding, and sustained immune dysregulation highlighting the need for careful oversight of these patients.

Highlights

- Consensus COVID-19 immune signature between solid cancer and non-cancer patients
- Resolution of immune dysregulation and sustained seroconversion in solid cancers
- Delayed or absent humoral responses observed in hematological cancer patients
- Prolonged viral clearance and post-virus immune legacy in hematological cancers

Article

Acute immune signatures and their legacies in severe acute respiratory syndrome coronavirus-2 infected cancer patients

Sultan Abdul-Jawad,^{1,26} Luca Baiù,^{2,26} Thanussuyah Alaguthurai,^{1,3,26} Irene del Molino del Barrio,^{4,5} Adam G. Laing,^{5,27} Thomas S. Hayday,^{5,27} Leticia Monin,^{6,27} Miguel Muñoz-Ruiz,^{6,27} Louisa McDonald,⁷ Isaac Francos Quijorna,⁸ Duncan McKenzie,⁶ Richard Davis,⁵ Anna Lorenc,⁵ Julie Nuo En Chan,¹ Sarah Ryan,⁹ Eva Bugallo-Blanco,¹ Rozalyn Yorke,⁹ Shraddha Kamdar,⁵ Matthew Fish,^{5,10} Iva Zlatareva,⁵ Pierre Vantourout,⁵ Aislinn Jennings,^{5,10} Sarah Gee,⁵ Katie Doores,¹¹ Katharine Bailey,¹² Sophie Hazell,¹² Julien De Naurois,¹³ Charlotte Moss,¹⁴ Beth Russell,¹⁴ Aadil A. Khan,¹⁵ Mark Rowley,^{16,17} Reuben Benjamin,^{1,18} Deborah Enting,¹⁴ Doraid Alrifai,¹³ Yin Wu,^{1,4,5,6} You Zhou,¹⁹

(Author list continued on next page)

¹School of Cancer & Pharmaceutical Sciences, King's College London, London, UK

²Institute of Biomedical Engineering, University of Oxford, Oxford, UK

³Breast Cancer Now Research Unit, King's College London, London, UK

⁴Cancer Immunotherapy Accelerator, UCL Cancer Institute, University College and King's College, London, UK

⁵Peter Gorer Department of Immunobiology, King's College London, London, UK

⁶The Francis Crick Institute, London, UK

⁷Oncology and Haematology Clinical Trials (OHCT), Guy's and St Thomas' NHS Foundation Trust, London UK

⁸Wolfson Centre for Age-Related Diseases, IoPPN, King's College London, London, UK

⁹Department of Inflammation Biology, King's College London, London, UK

¹⁰Department of Intensive Care Medicine, Guy's and St Thomas' NHS Foundation Trust, London, UK

¹¹Department of Infectious Diseases, King's College London, London, UK

¹²Department of Haematology, Guy's and St Thomas' NHS Foundation trust, London, UK

¹³Department of Medical Oncology Guy's and St Thomas' NHS Foundation Trust, London, UK

¹⁴Department of Translational Oncology & Urology Research (TOUR), King's College London, London, UK

¹⁵Targeted Therapy Team, The Institute of Cancer Research, London, UK

¹⁶London Institute for Mathematical Sciences, Mayfair, London, UK

¹⁷Saddle Point Science Ltd, London, UK

(Affiliations continued on next page)

SUMMARY

Given the immune system's importance for cancer surveillance and treatment, we have investigated how it may be affected by SARS-CoV-2 infection of cancer patients. Across some heterogeneity in tumor type, stage, and treatment, virus-exposed solid cancer patients display a dominant impact of SARS-CoV-2, apparent from the resemblance of their immune signatures to those for COVID-19+ non-cancer patients. This is not the case for hematological malignancies, with virus-exposed patients collectively displaying heterogeneous humoral responses, an exhausted T cell phenotype and a high prevalence of prolonged virus shedding. Furthermore, while recovered solid cancer patients' immunophenotypes resemble those of non-virus-exposed cancer patients, recovered hematological cancer patients display distinct, lingering immunological legacies. Thus, while solid cancer patients, including those with advanced disease, seem no more at risk of SARS-CoV-2-associated immune dysregulation than the general population, hematological cancer patients show complex immunological consequences of SARS-CoV-2 exposure that might usefully inform their care.

INTRODUCTION

For cancer patients, the coronavirus infectious disease 2019 (COVID-19) pandemic, caused by severe acute respiratory syndrome coronavirus-2 (SARS-CoV-2), has challenged decision

making about shielding and delaying treatment, instituted on "best guess" consensus rather than evidence (Maringe et al., 2020; Russell et al., 2020a; Ueda et al., 2020). Cancer patients, being immunocompromised, are historically considered high-risk for infections, although coronavirus infections are not

Paul Barber,¹ Tony Ng,¹ James Spicer,¹ Mieke Van Hemelrijck,¹⁴ Mayur Kumar,²⁰ Jennifer Vidler,¹⁸ Yadamar Lwin,¹⁸ Paul Fields,^{1,12} Sophia N. Karagiannis,^{3,21,22} Anthony C.C. Coolen,^{15,16,17,23} Anne Rigg,¹³ Sophie Papa,^{1,13} Adrian C. Hayday,^{5,6,28} Piers E.M. Patten,^{1,18,24} and Sheeba Irshad^{1,3,13,25,29,*}

¹⁸Department of Haematological Medicine, King's College Hospital, London, UK

¹⁹Systems Immunity University Research Institute and Division of Infection and Immunity, Cardiff University, Cardiff, UK

²⁰Department of Gastroenterology, Princess Royal University Hospital, Kent, UK

²¹St. John's Institute of Dermatology, King's College London, London, UK

²²NIHR Biomedical Research Centre, and King's College London, London, UK

²³Department of Biophysics, Radboud University, Nijmegen, The Netherlands

²⁴Medical Research Council (MRC) Clinical Academic Research Partnership, London, UK

²⁵Cancer Research UK (CRUK) Clinician Scientist, London, UK

²⁶Joint first authorship

²⁷These authors contributed equally

²⁸Senior author

²⁹Lead contact

*Correspondence: sheeba.irshad@kcl.ac.uk

<https://doi.org/10.1016/j.ccell.2021.01.001>

associated with more severe disease in the immunocompromised (Gralinski and Baric, 2015; Prompetchara et al., 2020; Xu et al., 2020). Attenuation of immune responsiveness may, indeed, be advantageous in COVID-19. Some COVID-19 clinical studies indicate poorer outcomes for cancer patients, especially those with hematological cancers (Pinato et al., 2020; Shah et al., 2020; Vijenthira et al., 2020; Williamson et al., 2020), but not others (Lee et al., 2020; Russell et al., 2020b). Insight into the impact of SARS-CoV-2 on cancer patients' immune status is lacking.

Immunological studies of hospitalized SARS-CoV-2 patients show hyper-inflammatory responses in about 25%–30% of cases (Huang et al., 2020; Laing et al., 2020). A consensus COVID-19 immune signature of a triad of interleukin (IL)-6, IL-10, and IP-10; selective T cell subset activation, exhaustion, and depletion; and substantial changes in dendritic cell, basophil, and B cell composition, likely contributing to COVID-19 pathology is present (Laing et al., 2020; Mathew et al., 2020). Whether and how this signature is impacted on by cancer and/or its treatment and vice versa is important (Russell et al., 2020a).

To address these issues, we established the SOAP study (Sars-CoV-2 fOr cAnCER Patients), which ran alongside the COVID-ImmunoPhenotyping (COVID-IP) (Laing et al., 2020), facilitating direct comparative analysis with non-cancer COVID-19+ and healthy controls (HC). We aimed to answer: (1) is there an immune signature of COVID-19 in cancer patients; and (2) do recovered cancer patients carry a post-infection immunological legacy? In addition, we would have the opportunity to assess the immune status of several patients who remained pauci-symptomatic or asymptomatic.

RESULTS

Cancer progression and prolonged viral persistence among COVID-19+ cancer patients

SOAP recruited 41 (23 solid and 18 hematological) patients confirmed as SARS-CoV-2 positive on nasopharyngeal swabs and 35 non-virus-exposed cancer controls (Table 1). We matched the exposed and non-exposed cancer patients for age (mean: 64 versus 57), BMI (24.8 versus 27.0) and tumor type; both cohorts included hematological and solid cancers. There was cross-cohort balance for cancer stage (stage IV dis-

ease: 55.9% versus 50%), treatment paradigm (radical intent: 31.7% versus 40%; palliative intent: 41.5% versus 48.6%) and receiving cancer treatment within 4 weeks of study recruitment: 47.9% of COVID-19+ solid cancer patients versus 53.8% of solid cancer controls; 50% of COVID-19+ hematological cancer patients versus 45.5% of hematological controls. A single lung cancer patient on immune checkpoint inhibitor (ICI) therapy was asymptomatic for COVID-19 and achieved a partial cancer treatment response 2 months after virus clearance. Overall, study cohorts were heterogeneous by design, captured traits broadly applicable to cancer, being well balanced between virus-exposed and non-exposed (Table 1).

Ten (24.4%) exposed cancer patients remained asymptomatic, 9 (21.9%) displayed mild, 13 (31.7%) moderate, and 9 (21.9%) severe disease (Figures 1A and S1A). Tumor subtypes were balanced across asymptomatic cases, but hematological cancers were enriched as severity scores increased (Figure 1A). Many patients did not require hospitalization and isolated at home until either asymptomatic/negative for COVID-19 by real-time RT-PCR (rRT-PCR) swab test (Figure 1B). COVID-19+ hematological patients showed fever and dyspnea, whereas COVID-19+ solid cancer patients experienced less dyspnea (Table S1). Seven (39%) hematological cancer patients received corticosteroid/antiviral therapies specifically for COVID-19. Overall 30-day mortality for the COVID-19+ cancer cohort was 21.9% (9 patients) with three deaths due to COVID-19 and 6 reflecting cancer progression (Figure 1B and Table 1).

We reviewed cancer status at 2 months after either first positive test (COVID-19+ cohort) or study entry date (non-COVID-19 cohort), for patients surviving beyond 30 days (n = 67/76). For 46 patients (COVID-19+ and non-COVID-19) with data, we found cancer disease progression to correlate significantly with prior COVID-19 severity status (Figure 1C). Thus, patients with moderate/severe COVID-19 were more likely to be diagnosed with progressive cancer at next clinical assessment, compared with those with either asymptomatic COVID-19 or non-exposed to SARS-CoV-2.

We next asked whether cancer impacted on progression of SARS-CoV-2 infection. Serial nasopharyngeal swab-tests were performed in 35 of 41 COVID-19+ cancer patients (Figure 1D) until a negative swab result (available for 33/35 patients, with two deaths during follow-up). Compared with a 12–20 day range in

Table 1. Clinical characteristics of the COVID-19+ and non-COVID-19 cancer cohort

	COVID-19+ Cancer (n = 41)	Non-COVID-19 Cancer Controls (n = 35)
Age		
Median	64	57
Range	(21–91)	(24–84)
Sex		
Male	24 (59%)	11 (32%)
Female	17 (41%)	23 (68%)
Race		
Caucasian	28 (68.3%)	20 (55.8%)
BAME	13 (31.7%)	14 (44.1%)
BMI		
Median	24.8	27
Range	15.8–41.9	17.29–39.25
Non-oncological comorbidities		
Cardiovascular disease (IHD, HTN, hypercholesteremia)	16 (39%)	7 (20%)
Diabetes	5 (12.2%)	4 (11.4%)
Underlying lung pathology	4 (9.7%)	3 (8.6%)
Cardiovascular disease	4 (9.7%)	3 (8.8%)
None of above	17 (41.5%)	22 (62.9%)
Oncological clinical history		
Solid malignancies	23/41 (56.1) (%)	26/35 (74.3%)
Women's cancers	6/23 (26.08%)	13/26 (50%)
Urological cancers	7/23 (30.43%)	5/26 (19.23%)
GI cancers	7/23 (30.43%)	4/26 (15.4%)
Lung & H&N cancers	3/23 (13.04%)	3/26 (11.5%)
Hematological Malignancies	18/41 (43.9%)	9/35 (25.7%)
Lymphomas	11/18 (61.11%)	4/9 (55.6%)
Diffuse large B cell lymphoma	9	4
Burkitt's lymphoma	1	-
Lymphoplasmacytic lymphoma	1	-
Leukemia type	6/18 (33.3%)	5/9 (44.4%)
Acute lymphocytic leukemia	3	1
Chronic lymphocytic leukemia	2	4
MDS/MPN	1	-
Myeloma	1/18 (5.56%)	-
Cancer Stage (Solid cancer and lymphomas only)	n = 34	n = 30
1	3 (8.8%)	5 (16.7%)
11	3 (8.8%)	2 (6.7%)
111	6 (17.6%)	8 (26.7%)
1V	19 (55.9%)	15 (50%)
Missing data	3 (8.8%)	0
Time from cancer diagnosis to study recruitment		
<3months	9 (22%)	8 (22.8%)
3–12 months	10 (24.3%)	9 (25.7%)
12–24 months	5 (12.2%)	7 (20%)
>24 months	17 (41.5%)	11 (31.4%)
ECOG Performance Status		
PS 0 or 1	16/41 (39.0%)	24/35 (68.6%)

(Continued on next page)

Table 1. Continued

	COVID-19 ⁺ Cancer (n = 41)	Non-COVID-19 Cancer Controls (n = 35)
PS 2	14/41 (34.1%)	3/35 (8.6%)
PS 3 or 4	2/41 (4.9%)	2/35 (5.7%)
Unknown	9/41 (22%)	6/35 (17.1%)
Treatment paradigm at the time of COVID-19 ⁺ presentation		
Treatment naive	7 (17.1%)	2 (5.7%)
Radical (<i>Primary Surgery, Neoadjuvant, Adjuvant</i>)	13 (31.7%)	14 (40%)
Palliative	17 (41.5%)	17 (48.6%)
Watch and wait/Surveillance	3 (7.3%)	1 (2.9%)
Missing data	1 (2.4%)	1 (2.9%)
Final anti-cancer treatments (<i>excluding treatment naive patients/missing data</i>)		
Time from study blood draw: median (range) days	27 (1–569)	22 (2–904)
Time from COVID-19 ⁺ presentation: median (range) days	30 (0–564)	NA
Anti-cancer treatment in the 4 weeks before study blood drawn		
Solid cancers		
No treatment within this time frame	13/23 (52.1%)	12/26 (46.2%)
Chemotherapeutic agents	4	7
Radiotherapy	2	1
Chemo-RT	0	1
Targeted therapies	3	3
Immunotherapies	1	2
Missing data	0	0
Hematological cancers		
No treatment within this time frame	9/18 (50%)	4/9 (55.5%)
Anti-CD20 monoclonal antibody therapy	3	2
Immune-modulators (e.g., Lenalidomide)	2	1
Targeted agents (e.g., BTKi)	2	1
Chemotherapeutic agents	6	3
Anti-cancer treatment in the 4 weeks before COVID-19 ⁺ presentation		
Solid cancers		
No treatment within this time frame	17/23 (73.9%)	
Chemotherapeutic agents	3	
Radiotherapy	1	
Targeted therapies	1	
Immunotherapies	1	
Hematological cancers		
No treatment within this time frame	8/18 (44.5%)	
Anti-CD20 monoclonal antibody therapy	3	
Immune-modulators (e.g., Lenalidomide)	2	
Targeted agents (e.g., BTKi)	2	
Chemotherapeutic agents	6	
Stem-cell transplant ^a (within 12 months)	1	
Bendamustine* (within 12 months)	1	
Concomitant immunomodulatory drugs		
Nonsteroidal anti-inflammatory drugs		
Yes	5/41 (12.2%)	3/35 (8.6%)
No	32/41 (78%)	28/35 (80%)

(Continued on next page)

Table 1. Continued

	COVID-19 ⁺ Cancer (n = 41)	Non-COVID-19 Cancer Controls (n = 35)
Missing data	4/41 (9.8%)	4/35 (11.4%)
High-dose steroids		
Yes	19/41 (46.3%)	9/35 (25.8%)
No	20/41 (48.9%)	25/35 (82.9%)
Missing data	2/41 (4.9%)	1 (2.9%)
30-Day all-cause mortality	From first positive swab test	From study entry
No	32/41 (78.0%)	35/35 (100%)
Yes	9/41 (22.0%)	0/35 (0%)
COVID-19 mortality	3/9 (33.3%)	
Cancer progression mortality	6/9 (66.7%)	

Related to [Figures 1](#) and [S1](#) and [Table S1](#).

^aAnti-cancer treatment within 12 months of SARS-CoV-2 exposure.

non-cancer patients ([He et al., 2020](#); [Young et al., 2020](#)), RNA persistence beyond 20 days was seen in 60% of hematological and 35% of solid cancer patients ([Figure 1D](#)), with a median duration of virus shedding (interval between first and last positive test) of 39 days (range 7–107) (hematological: median, 55, range 7–90; solid: median 29, range 22–107). Interestingly, the COVID-19⁺ solid cancer patient showing swab test positivity until day 107 remained asymptomatic.

Clinical blood parameters of COVID-19⁺ cancer patients

We asked if SOAP resembled COVID-19 in the general population where several clinical and/or laboratory blood parameters correlate with COVID-19 severity. Presentation total white blood cell, neutrophil, and platelet counts were similar between cancer cohorts ([Figure S1B](#), i–iii), although COVID-19⁺ patients had reduced lymphocyte and basophil counts, with elevated neutrophil-to-lymphocyte ratios (NLR) and platelet-to-lymphocyte ratios (PLR) ([Figure S1B](#), vi–vii). Correlation analyses identified NLR, PLR, basophil and lymphocyte counts, albumin, and hemoglobin as significant positive or negative correlates of COVID-19 severity ([Figure 1E](#)); lymphopenia and hypoalbuminemia had the highest predictive accuracy ([Figures 1F](#) and [1C](#)). Eighty percent of COVID-19⁺ cancer patients assessed for CRP showed elevated levels (median 185.1 mg/L) ([Figure S1D](#), i). Serum ferritin was elevated in 96% of cases (median 1335 mg/L), and D-dimer was elevated in severe cases (median 9.22 ng/mL) ([Figure S1D](#), ii–iii). There were no significant differences between blood parameters when stratified by ethnicity, BMI, immunomodulatory therapy (steroids and nonsteroidal anti-inflammatory drugs), or administration of active cancer treatment within 4 weeks of COVID-19 presentation in solid ([Figure S1E](#)) and hematological ([Figure S1F](#)) cancers, consistent with the cohort examined as a whole (see [Figure 1E](#)). The only significant correlations were of blood albumin with gender and age ([Figure 1E](#)).

Longitudinal profiling of actively infected and recovered SARS-CoV-2⁺ cancer patients

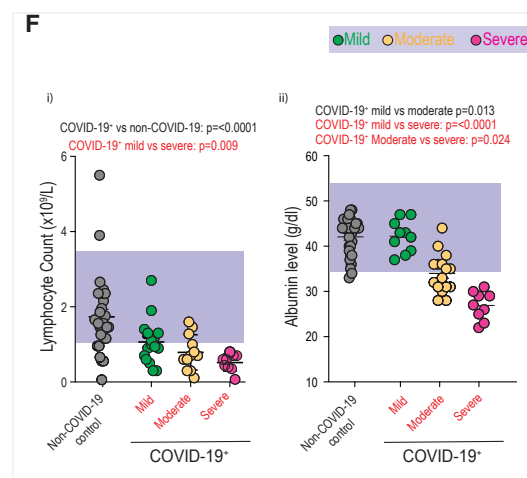
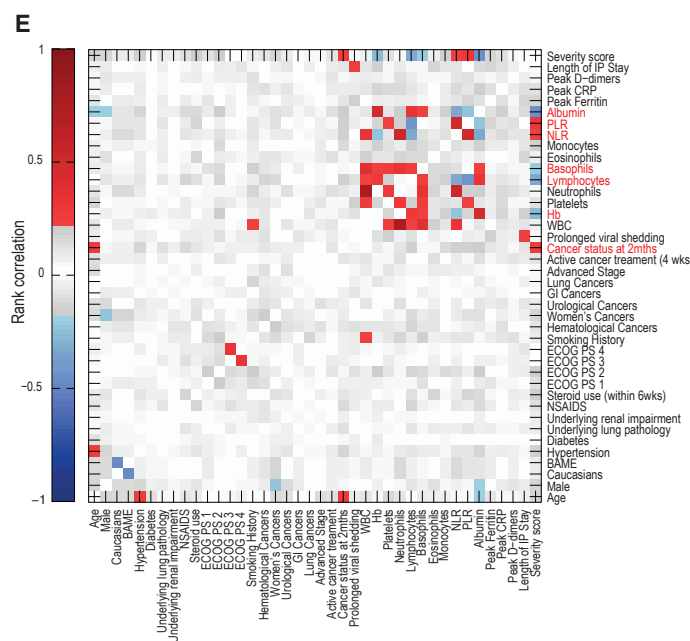
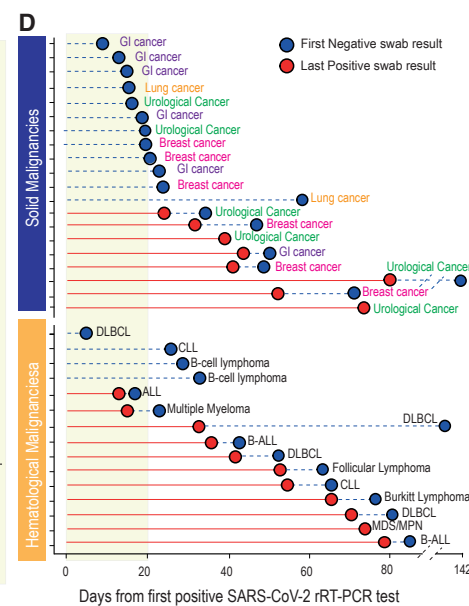
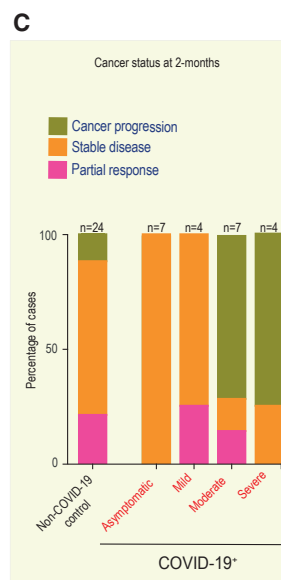
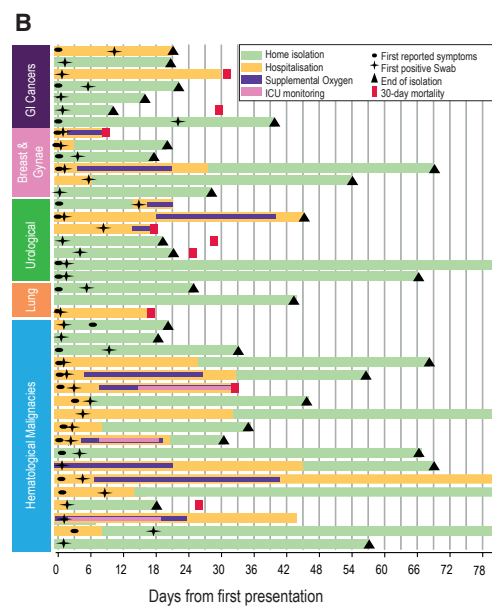
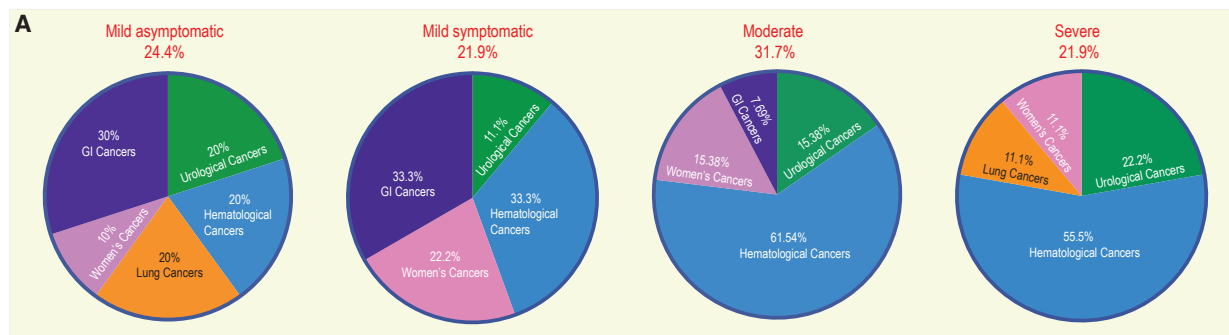
We next undertook longitudinal analyses of clinical blood parameters ([Figure 2A](#)). Patients were stratified by solid versus hematological cancer and mild versus moderate/severe COVID-19. Solid cancer patients with moderate/severe disease commonly

showed sustained lymphopenia and increased NLR while actively infected up to day 40–49 (Wilcoxon rank-sum test, p values: 5.16×10^{-5} , 3×10^{-4} , respectively), particularly as lymphocytes showed negligible recovery while neutrophilia became more evident (Wilcoxon rank-sum test, p value = 0.008) ([Figure 2B](#)). Basophil counts likewise remained low ([Figure S2A](#), ii). Conversely, measurements for counterpart patients with mild COVID-19 were commonly in the normal range set, albeit with some considerable variability in basophil and eosinophil counts ([Figures 2B](#) and [S2A](#)). While actively infected COVID-19⁺ hematological cancer patients showed similar longitudinal profiles to COVID-19⁺ solid cancer patients, their deviations from normal were collectively less, albeit variable, and those with mild and moderate/severe COVID-19 showed largely overlapping trajectories ([Figures 2C](#) and [S2B](#)).

No leukocyte parameter trajectories were affected by either administration of cytotoxic agents ([Figure S2C](#)) or anti-CD20 monoclonal antibodies (mab) ([Figure S2D](#)) within 4 weeks of COVID-19 presentation ([Table S2](#)). Conversely, lymphopenia and increased NLR, at presentation (days 0–3) were predictive of subsequent cancer progression measured at 2 months (Wilcoxon rank-sum test, p values: 0.009 and 0.004, respectively) ([Figure S2E](#)).

We next asked whether the *status quo* would be reestablished at between 1 and 2 months post-infection, signaled by a negative SARS-CoV-2 swab test; comparing points of peak dysregulation during active infection and at 4–6 weeks before and 4–6 weeks after COVID-19 exposure (see [Figure 2A](#)). COVID-19⁺ solid cancer patients during active infection exhibited significant reductions in lymphocyte and monocyte counts compared with pre-COVID-19 levels (Wilcoxon signed rank test, p = 0.003 and 0.006, respectively) with resultant increases in NLR and PLR (Wilcoxon signed rank test, p = 0.004 and 0.006, respectively) ([Figure 2D](#), i). COVID-19⁺ hematological cancer patients displayed similar results (Wilcoxon signed rank test, p = 0.009, 0.02, 0.02, and 0.02, respectively) ([Figure 2D](#), ii), although there was higher interindividual variation in fold change over time, compared with solid cancer patients ([Figure 2D](#); compare y axes in i versus ii).

In COVID-19⁺ solid cancer patients, all parameters returned close to basal values by 4–6 weeks after a negative swab ([Figure 2E](#), i; compare with [Figure 2Di](#)). By contrast, the



(legend on next page)

interindividual variability of hematological cancer patients persisted with many patients exhibiting ongoing dysregulation (Figure 2E, ii). No significant differences were observed when stratified by ethnicity, BMI, immunomodulatory therapy, or active cancer treatment within 4 weeks of COVID-19 presentation (Tables S2 and S3).

Distinct COVID-19 immune signatures in solid and hematological cancer patients

To understand leukocyte dysregulation in COVID-19⁺ cancer, we used eight flow cytometry panels (P1–P8) to measure: (1) broad lymphocyte composition; (2) effector/memory T cell status; (3) $\gamma\delta$ T cell status; (4) B cells; (5) T cell cycling; (6) leukocyte counts; (7) lymphocyte activation and exhaustion; and (8) innate immune cells (Laing et al., 2020). We compared COVID-19⁺ cancer patients ($n = 41$) with control groups comprising non-COVID-19 cancer patients ($n = 35$), COVID-19⁺ non-cancer patients ($n = 52$), COVID-19 seropositive recovered HC ($n = 22$), and seronegative HC ($n = 46$). Samples were grouped into “active” infection (blood sample <14 days of positive rRT-PCR swab test) or “recovered” (blood sample after a negative rRT-PCR swab test, and for non-cancer HC by immunoglobulin (Ig)G/IgM serology status). Therefore, we could identify the most significant changes precipitated by COVID-19 in solid or hematological cancer patients versus their non-COVID-19 cancer controls and HC (Figure 3A), during both the active and recovered phases of infection.

We used principal component analysis (PCA) to examine 175 immune flow cytometry parameters and 22 cytokines across the groups (Figure 3B and S3A). Hematological (Figure 3B, yellow dots) and solid COVID-19⁺ cancer patients (Figure 3B, blue dots) segregated from each other, supporting the decision to consider these two groups separately to be compared with their respective controls (Figure 3A). We observed that active COVID-19⁺ cancer patients segregated from their non-COVID-19 cancer controls, just as active COVID-19⁺ non-cancer subjects segregated from HC (Figure S3A, i). By contrast, immune profiles of recovered patients overlapped with their respective control groups (Figure S3A, ii), consistent with the analysis of their clinical blood parameters.

The covariates significantly distinguishing active SARS-CoV-2⁺ solid cancer patients from their non-COVID-19 solid cancer controls, included several parameters previously identified as composing a COVID-19 immune signature in non-cancer patients (Laing et al., 2020; Mathew et al., 2020), e.g. IL-8, IL-6, and IL-10, IP-10 enrichment; T cell activation (HLA-DR, CD38; G1-cycling) and exhaustion (TIM3⁺PD1⁺); and decreased baso-

phils (Figure 3C). In contrast, COVID-19⁺ hematological cancer patients showed fewer discrete changes compared with hematological cancer controls, with the most overt changes being increased frequencies of CD8⁺ T cells with active cycling and exhaustion markers, increased CD56^{hi} NK cells, and reduced B cell counts (Figure 3D).

In the recovery phase, the high-content analysis showed that only CD8⁺ V δ 1⁺ $\gamma\delta$ T cells significantly distinguished recovered SARS-CoV-2⁺ solid cancer versus its controls (Figure 3E). In separate studies (A.H., unpublished data) we have found that COVID-19⁺ non-cancer patients display strong, clonally restricted expansions of CD8⁺ V δ 1⁺ $\gamma\delta$ T, consistent with this being a sustained immunological legacy. In stark contrast, the collective failures of recovered hematological cancer patients to re-normalize their clinical blood parameters was underpinned by significant differences in many adaptive lymphocytic and innate myelomonocytic parameters between post-infection hematological cancer patients and their non-COVID-19 controls (Figure 3F).

The COVID-19 associated immunophenotypes of asymptomatic and symptomatic patients were comparable, in that they could not be segregated in a PCA of 62 immune parameters (Figure S3B). There were two outliers with distinct immunophenotypes: (1) the asymptomatic patient on active ICI anti-PD1 therapy (Figure S3B; arrow); and (2) a symptomatic lymphoma patient with prolonged virus shedding (day 66).

We next showed that this strong, yet mostly transient, COVID-19 immune signature in solid cancer patients differed from COVID-19⁺ non-cancer signatures by exaggerated elevation of IL-6/IL-10 and cytopenia in defined B, T, NK, and DC subsets (Figure S3C). These findings likely reflect inherent differences in the baseline immune milieu of cancer patients and non-cancer subjects. Conversely, the immune landscapes of COVID-19⁺ hematological cancer patients and COVID-19⁺ non-cancer subjects most clearly segregated by different criteria including increased CD56^{hi} NK cell frequency, T cell activation/exhaustion, and exaggerated B cytopenia (Figure S3D).

To probe further how either solid cancer or hematological cancer may modify the effect of COVID-19 on various immune parameters, we looked for interaction effects that were either synergistic or antagonistic, by asking whether the fold changes in the COVID-19⁺ cancer cohorts versus HC were significantly > or < than expected when the fold changes of COVID-19⁺ versus HC or cancer versus HC were considered separately. Evidence of interactions was only found in SARS-CoV-2 active patients, predominantly in the solid cancer cohort: synergistic interaction effects included interferon

Figure 1. Cancer progression and prolonged viral persistence among COVID-19⁺ cancer patients

(A) Stratification of COVID-19 severity groups by cancer type.

(B) Timeline of illness of 41 COVID-19⁺ cancer patients by tumor type.

(C) Stacked bar graph shows the disease status of cancer in patients grouped according to COVID-19 severity. Association between categorical variables was assessed by chi-squared test ($p < 0.001$).

(D) Timeline of detection of SARS-CoV-2 on nasopharyngeal swabs. Day 1 indicates collection date of the earliest positive sample. Blue dots mark the date of the earliest negative rRT-PCR test; red dots the latest sample tested positive. The shaded area indicates the reported median duration of virus shedding.

(E) Correlation multivariate regression analysis of the clinical parameters within the cancer cohort (red = statistically significant correlations).

(F) i–ii, Quantification of significant parameters captured on clinical blood tests in COVID-19⁺ cancer patients; healthy ranges are indicated in purple. One-way ANOVA was used to compare continuous variable among three groups of severity, while independent samples t test was used between two groups (COVID-19⁺ versus non-COVID-19). $p < 0.05$ was considered statistically significant.

See also Figure S1 and Table S1.

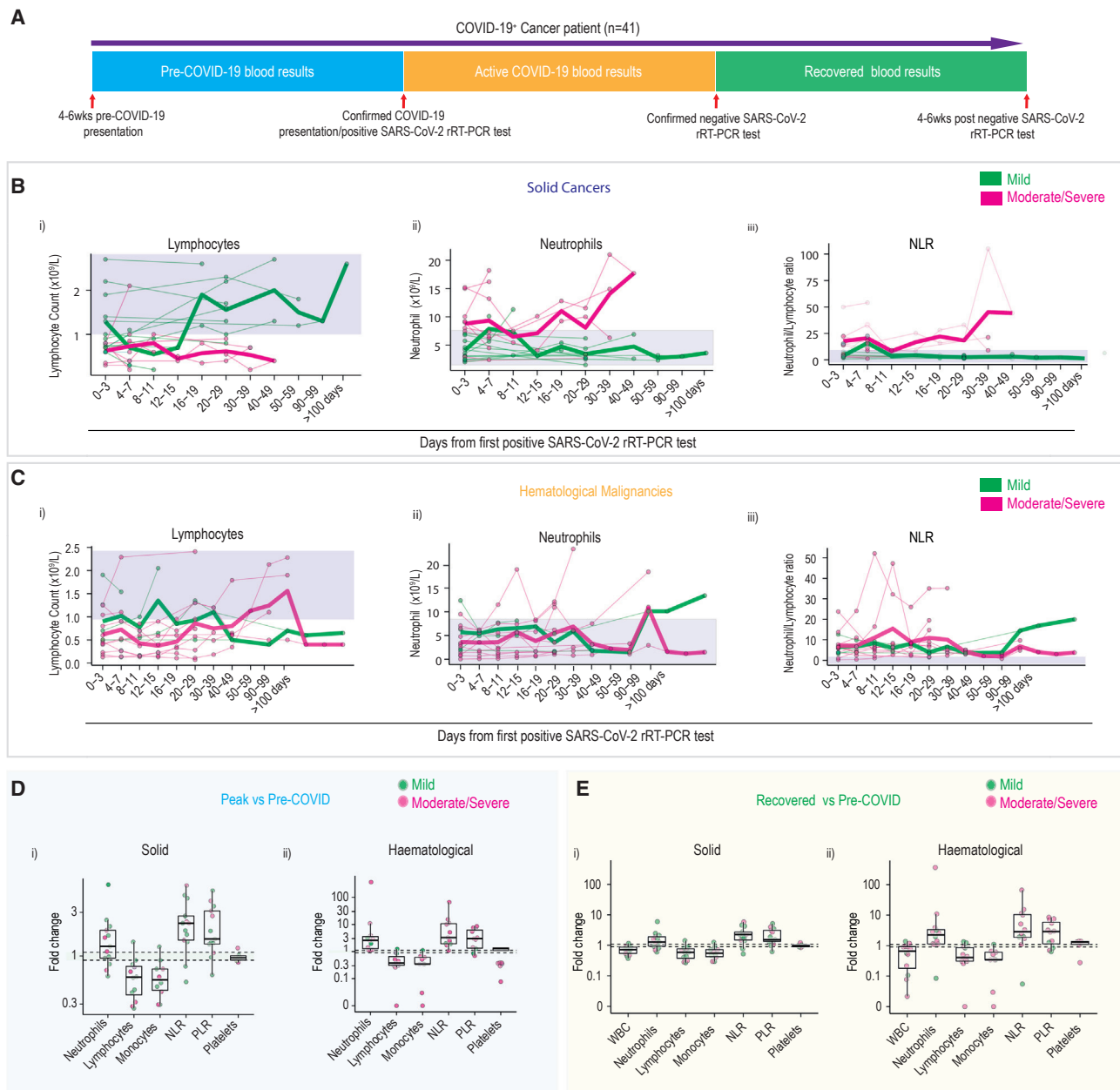


Figure 2. Longitudinal profiling of actively infected and recovered SARS-CoV-2+ patients

(A) Schematic of time points for blood results from 41 patients in the COVID-19+ cancer cohorts.

(B and C) Time course of (i) lymphocytes, (ii) neutrophils, (iii) neutrophil-to-lymphocyte ratio in active COVID-19 disease for solid (B) and hematological (C) cancer patients with mild World Health Organization (WHO) score (0–3) and moderate/severe illness, (WHO score 4–10). Points represent the median of each patient’s measurements in the corresponding time bin, thin lines connect measurements on the same patient, thick lines show the mean of all patients at each time point stratified by severity. Healthy ranges are highlighted in purple.

(D) Fold change of blood parameters for each solid (i) or hematological (ii) cancer patient between the time of worst abnormality and the pre-COVID blood tests 4–6 weeks prior to COVID-19 presentation.

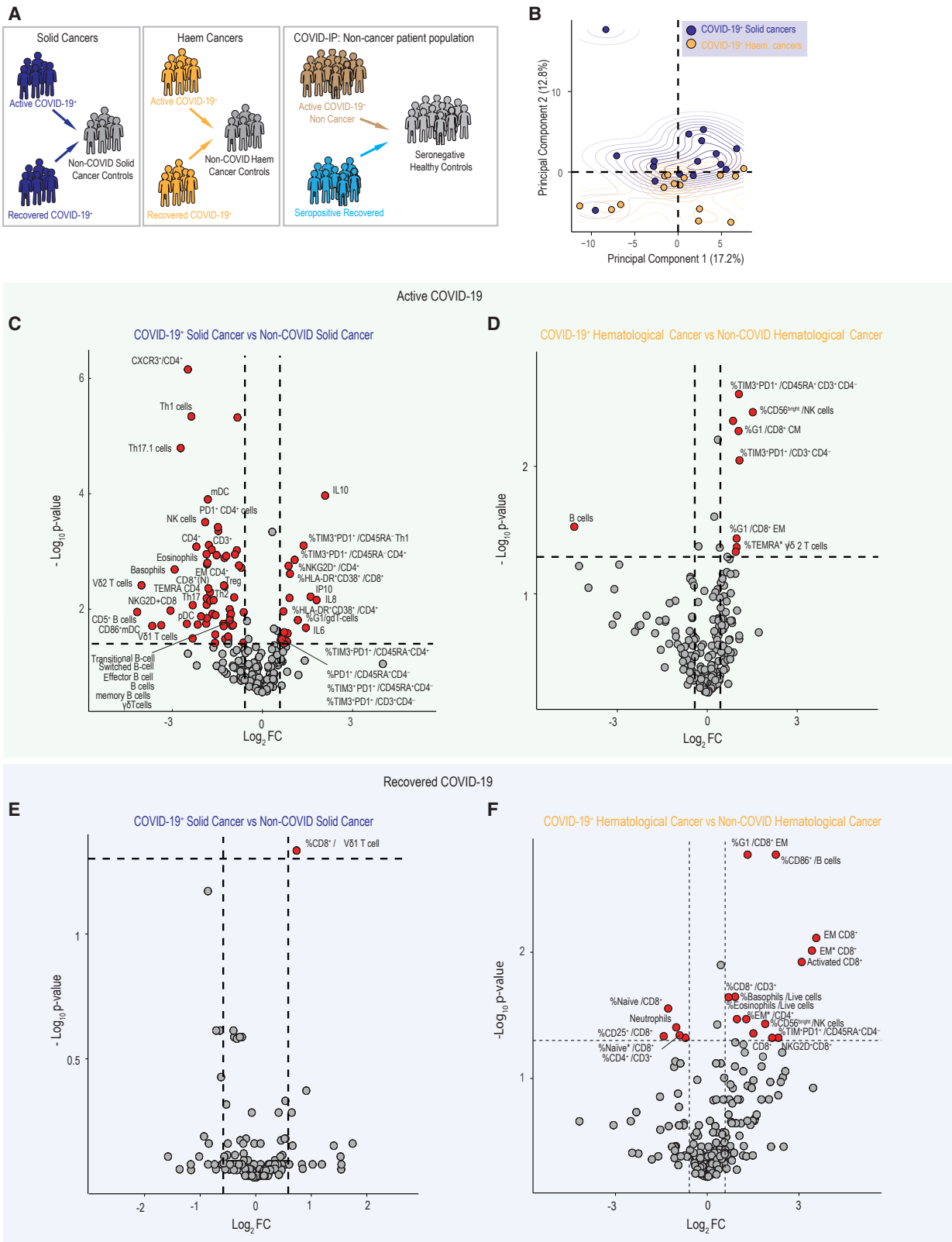
(E) Fold change of blood parameters for solid (i); hematological (ii) cancer patients between results after recovery and the last pre-COVID-19 results. Shaded area denotes measurements within 10% of pre-COVID levels.

See also [Figure S2](#) and [Tables S2](#) and [S3](#).

(IFN) γ -producing cytopenia (NK, Th1, Th17.1) while antagonistic interactions included T cell cycling, and none of these were included in the four antagonistic interactions observed for hematological cancers ([Figure S3E](#)).

Altered immune cell populations in actively infected SARS-CoV-2+ cancer patients

Consistent with the effect size analyses, reduced numbers of B, T, NK, and myeloid DC seen in COVID-19+ solid cancer subjects



(legend on next page)

were significantly exaggerated relative to COVID-19⁺ non-cancer subjects, and, with the exception of T cytopenia (see below), this commonly included patients presenting with mild COVID-19 (Figures 4A and S4A–B). Basophil and plasmacytoid DC counts were likewise low but comparable to COVID-19⁺ non-cancer subjects (Figures 4Aiv and S4Ai). The reduced eosinophil numbers in COVID-19⁺ solid cancer patients must be contextualized with atypically high eosinophil counts displayed by non-COVID-19 cancer controls (Figure 4Avi). Consistent with the overall complexion of immune dysregulation being comparable across symptomatic and asymptomatic COVID-19⁺ solid cancer patients, only reduced T cell and basophil counts correlated significantly with COVID-19 severity (Figure 4B), as they likewise did in COVID-19⁺ non-cancer patients (Laing et al., 2020).

In hematological malignancies, marked attrition of B cells was noted in COVID-19⁺ patients (Figure 4Ai). Two patients from the COVID-19⁺ group and two control patients in this analysis had received anti-CD20 mab within 28 days of study entry blood draw (specifically days 12, 19 in the COVID-19 group and days 1, 6 for the non-COVID-19 group) (Figure 4Ai; arrows). The underlying malignancy did not offer an explanation for B cytopenia, since the hematological cancer cohorts were well balanced, with all patients in the control group diagnosed with B cell malignancies and on similar treatments to the study cohort, with a single patient in the study cohort diagnosed with myelodysplastic syndrome (MDS) (Table 1). Note, this patient (64-year-old male) was a clear outlier for T cytopenia (Figure 4Aii; brown arrow), and was the one direct COVID-19 related mortality in the hematological cancer cohort (see Figure 1B). No other cell counts significantly segregated COVID-19⁺ hematological cancer patients from controls, in part because of the very high interindividual phenotypic variation of the COVID-19 cohort.

The high levels of selected chemokines and cytokines characteristic of non-cancer COVID-19⁺ subjects (Laing et al., 2020; Mathew et al., 2020; Yang et al., 2020) were evident in COVID-19⁺ solid cancer patients and were sometimes exaggerated. Indeed, in COVID-19⁺ solid cancer and non-cancer cohorts, upregulation of IP-10, IL-10, and IL-8 was correlated with COVID-19 severity, with which IL-6 was also upregulated (Figures 4C, 4D, and S4C). IL-6, IL-10, and IP-10 levels were also high in SARS-CoV-2⁺ hematological cancer patients but not significantly upregulated relative to their control cohort, in part because non-COVID-19 hematological cancer patients can also display highly elevated levels of these analytes.

T cell dysfunction in active SARS-CoV-2-infected cancer patients

We next examined the detailed T cell biology of SARS-CoV-2-exposed cancer patients. COVID-19⁺ solid cancers showed significantly reduced CD8⁺ T cell numbers (Figures 5A and S5A) and although most significant for naive CD8⁺ T cells, there

was a clear trend toward low counts for all CD8⁺ T cell subsets with the exception of T_{EMRA}, as previously reported for non-cancer COVID-19⁺ (Laing et al., 2020; Mathew et al., 2020; Wen et al., 2020) (Figures 5A, ii and S5A). Of note, counts for each subset were less overtly depleted for those with mild disease, including asymptomatic patients (Figures 5A and S5A).

Also similar to non-cancer COVID-19⁺, significant CD4⁺ T cytopenia was observed in COVID-19⁺ solid cancer patients, albeit with an exaggerated phenotype despite there being a higher prevalence of mild/asymptomatic patients in this study (Figure 5B). Whereas COVID-19⁺ solid cancer and non-cancer patients both displayed overt drops in effector memory CD4⁺ T cells, particularly severe COVID-19 cases, COVID-19⁺ solid cancer patients displayed exaggerated depletions among central memory cells and naive CD4⁺ T cells (Figure 5C and 5D), the latter correlating significantly with disease severity (Figure 5E). Further, we observed greater fold change decreases in IFN γ -producing Th1 and Th17.1 subsets compared with Th2, Th17, and Treg, albeit the latter populations were also decreased (Figures 5C and S5B). The exaggerated depletions noted for Th1 and Th17.1 reflect synergistic interactions between cancer and COVID-19, as identified in Figure S3Ei.

Given that T cell dysregulation in COVID-19⁺ non-cancer patients coexisted with marked T cell activation and exhaustion, we investigated these immune parameters in the cancer cohorts. This same phenomenon was observed in actively infected COVID-19⁺ solid cancer patients, evidenced by increased frequencies of HLA-DR⁺CD38⁺ activated CD4⁺ and CD8⁺ T cells (Figures 5F and S5C), and increased frequencies of TIM3⁺ and/or PD1⁺ expression among CD4⁺ and CD8⁺ T cells (Diao et al., 2020; Laing et al., 2020; Mathew et al., 2020; Sekine et al., 2020a, 2020b; Wen et al., 2020). Particularly affected were CD45RA⁻ CD4⁺, CD45RA⁻ Th1, and CD45RA⁺ CD4⁺ and CD8⁺ T cells (Figure 5G, 5H, and S5D).

A similar pattern was observed in hematological cancers, with upregulation of exhaustion markers on CD8⁺ T cells (Figure 5F), coupled with a trend toward increased CD8⁺/CD4⁺ T cell activation (Figure S5C), manifested as significantly higher frequencies of activated and exhausted CD4⁺ T cells in COVID-19⁺ compared with COVID-19⁺ non-cancer subjects (Figures S5C and S5D). These data provided a basis for the effect size analysis presented above (see Figure S3D).

Heterogeneous humoral responses to SARS-CoV-2 in cancer patients

The overt B cytopenia in active COVID-19⁺ solid cancer patients reflected significant reductions in the numbers of naive, memory (switched and non-switched), effector and transitional B cells (Figures 6A and S6A), and, as with COVID-19⁺ non-cancer patients, there were significant reductions in the frequencies and numbers of CD5⁺ B cells that are primary producers of self-reactive and

Figure 3. Distinct COVID-19 immune signatures in solid and hematological cancer patients

(A) Overview of the nine patient cohorts grouped according to cancer type and COVID-19 status.
(B) PCA analysis of 153 phenotypes in 31 COVID-19⁺ cancer patients. PC-1 and PC-2 explain 17.2% and 11.9% of the variance.
(C–F) Volcano plot of 246 non-redundant immune parameters analyzed in active COVID-19⁺ (C) solid; (D) hematological cancer; recovered COVID-19⁺ (E) solid; (F) hematological cancers versus their respective non-COVID-19 cancer controls. Red circles = significantly altered parameters in COVID-19⁺ cancer patients (fold change >1.5, false discovery rate-adjusted $p < 0.05$).
See also Figure S3.

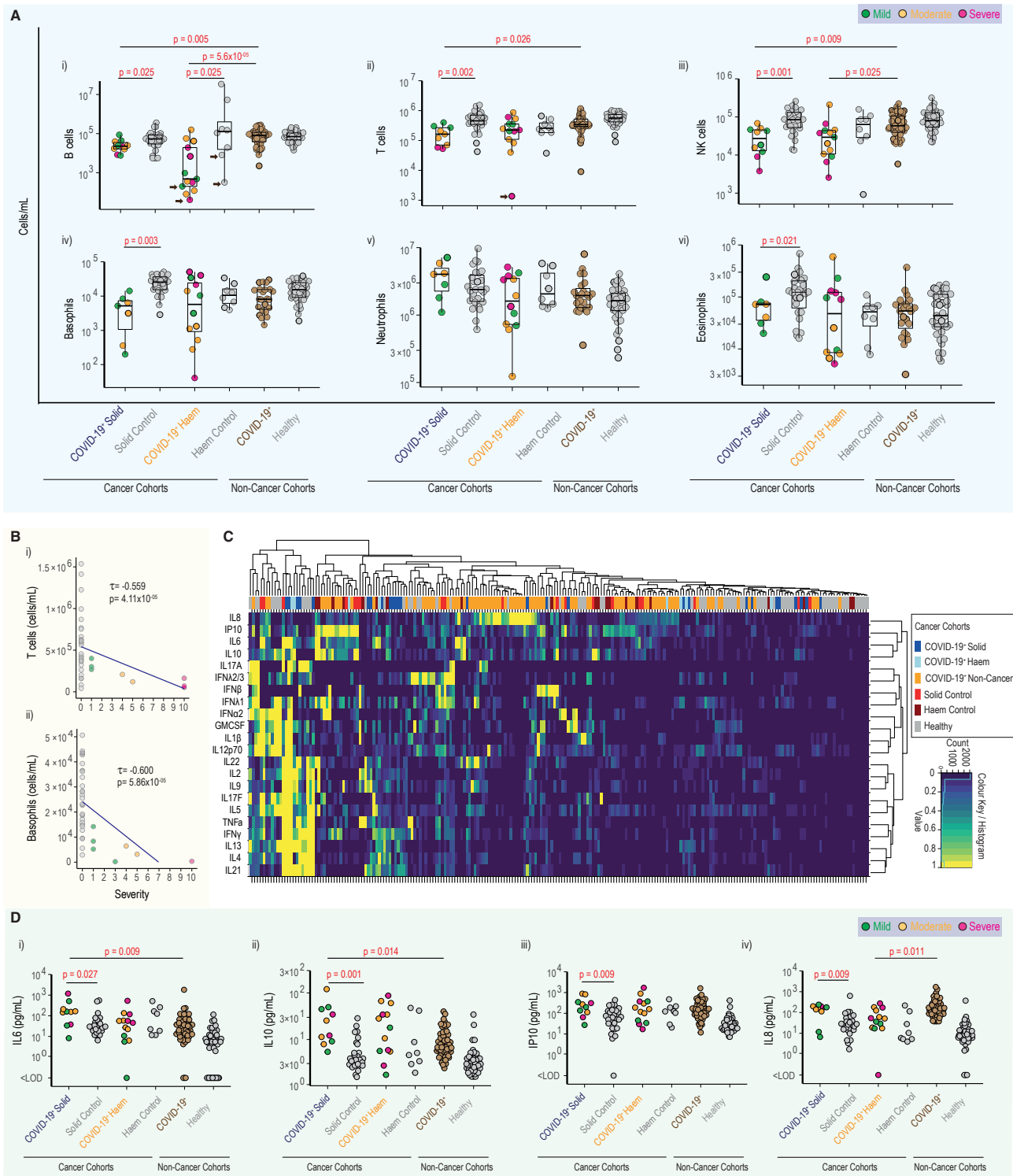


Figure 4. Altered immune cell populations in actively infected SARS-CoV-2+ cancer patients

(A) i–vi, Quantification (cell counts/mL) of whole blood major innate and adaptive immune populations.

(B) Correlation between (i) T cells; (ii) Basophil cell counts and COVID-19 severity in actively infected solid cancer patients (Kendall's tau for semi-partial correlation; adjusted for age and sex).

(C) Quantile scaled heatmap depicting hierarchical clustering of relative cytokine levels (quantile scaled pg/mL) 22 unique cytokines measured in six cohorts.

(legend continued on next page)

polyreactive natural antibodies (Figures 6A and S6A, vi-B, vi). Across the COVID-19+ solid cancer cohort, plasmablast numbers were not significantly increased relative to non-COVID-19 solid cancer controls (Figure S6A, v), most likely reflecting the longer time course of COVID-19 in these patients set against the known transience of plasmablast expansions. B cytopenia was particularly overt in COVID-19+ hematological cancer patients (Figure 6A), but owing to the high interindividual variation in that group and their controls, naive B cells were the only subset consistently depleted (Figure S6A).

Despite the overt dysregulation of monocytes, B and T cells in COVID-19+ cancer patients, many patients successfully developed IgM/IgG antibodies to SARS-CoV-2 receptor binding domain (RBD), Spike (S), and nucleocapsid antigens (N) (Figure 6B and Table S4). Antibodies were measured from time to first positive COVID-19 rRT-PCR test in 22 of 23 solid cancer patients and 16 of 18 hematological cancer patients; longitudinal analyses were possible in 11 cases, denoted by connected lines (Figure 6B). Anti-RBD IgM and IgG titers correlated with each other, as did anti-Spike IgM and IgG titers in active COVID-19+ cancer patients, but this was not true in recovered patients (Figure S6C).

Although ~75% of the COVID-19+ cancer patients had detectable antibodies against SARS-CoV-2 spike protein (31 of 41 IgG [total]; 28 of 41 IgM [total]) (Figure 6B), we noted several distinct features. First, COVID-19+ solid cancers showed earlier seroconversion than COVID-19+ hematological cancer patients (Figure 6B; compare blue with yellow circles above the threshold line). Second, all solid cancer patients with subsequent negative rRT-PCR swab-tests seroconverted for anti-Spike IgG, with the single exception (Figure 6B; arrowed) of a patient diagnosed with stage 4 colorectal cancer, on active triple therapy (anti-EGFR mab antibody, MEK inhibitor, and BRAF inhibitor) presenting with low-severity COVID-19.

Third, COVID-19+ hematological cancer patients showed three phenotypes: (1) patients failing to mount an antibody response with prolonged viral shedding, even beyond day 50 from first positive swab (Figure 6B; yellow circles below the seroconversion threshold line); (2) patients mounting an antibody response but failing to clear virus (Figure 6B; yellow circles above the threshold line); and (3) those able to mount an antibody response and successfully clear virus, as confirmed by a negative rRT-PCR test (Figure 6B; yellow triangles above the seroconversion threshold line). The five hematological cancer patients who remained positive for SARS-CoV-2 on rRT-PCR testing (beyond 20 days) and lacked subsequent seroconversion had received treatments likely to result in B cell aplasia. Three had received anti-CD20 mab within 4 weeks (8, 13, and 23 days) prior to their first positive swab; one was an MDS/MPN patient who had had an allograft (including conditioning with anti-CD52) ~7 months prior to COVID-19 presentation, receiving high-dose steroids at the time of COVID-19 presentation for graft versus host disease; one had received cytarabine, etoposide, methotrexate, and imatinib treatment for B-ALL 1 day prior to COVID-19 presentation.

IgM and IgG antibody titers of patients with either solid or hematological malignancies were comparable with those of COVID-19+ non-cancer patients (Figure 6C). Compared with COVID-19+ non-cancer subjects, S-reactive and RBD-reactive IgG were both significantly increased in hematological cancer patients recovered from SARS-CoV-2 infection (Figure 6D), likely reflecting the delayed peaking of the antibody responses observed in those patients (see Figure 6B).

Immune legacies in recovered COVID-19+ hematological cancer patients

To answer whether or not immune responses to SARS-CoV-2 exposure left a lasting legacy influencing immune surveillance of cancer, we examined the immune profiles of COVID-19+ patients following a negative rRT-PCR swab test. Median analysis time following recovery was 38.5 and 43 days in solid and hematological cancers, respectively (Figure S7A). Strikingly, the immune profiles in solid cancer COVID-19+ patients displayed minimal immune legacy of SARS-CoV-2, the only significant, albeit small, fold change was in CD8⁺Vδ1⁺ γδ T cells (Figure 7A). The patient on anti-PD-1 therapy appeared as a sustained outlier with low cell counts for T cell subsets such as Th17, Th2, central and effector memory, as well as low PD-1 expression on CD4 and CD8 T cells (Figure S7B; red circles), consistent with anti-PD-1 therapy.

In contrast, recovered patients with hematological cancers had several significantly altered immune parameters (Figure 7A). There were consistently increased CD8⁺ counts, irrespective of COVID-19 severity (Figure 7B, i), and the frequency of these cells among T cells also increased (Figure S7C, i) given that there was no parallel expansion of CD4⁺ T cell counts and frequency (Figures 7B, ii and S7C, ii). The CD8⁺ T cell expansions were significant in the effector memory compartment with a similar trend for CD8⁺ CM cells (Figure 7C). The frequency of CD8⁺ cells expressing exhaustion markers (TIM3⁺ PD1⁺) with concurrent activation was increased (Figure 7D). Among CD4⁺ T cells, there was increased representation of EM cells, and a similar trend for CM cells (Figure S7D).

Post-infection COVID-19+ hematological cancer patients also showed significantly increased frequencies of basophils and eosinophils (Figure 7E, i and ii), two compartments commonly depleted in COVID-19 aligning with observations in some COVID-19+ non-cancer patient populations (Lucas et al., 2020; Rodriguez et al., 2020). Recovered hematological COVID-19+ cancer patients also showed a significant increase in the frequency of CD56^{bright} NK cells (Figure 7E, iii). These observations require further investigation in the context of ongoing cancer immune surveillance.

DISCUSSION

The impact of exposure to SARS-CoV-2 in cancer patients remains unclear (Kuderer et al., 2020; Lee et al., 2020). Our study cohort is inevitably heterogeneous, but despite this heterogeneity,

(D) Cytokine concentrations of (i) IL-6, (ii) IL-10, (iii) IP-10, (iv) IL-8. Boxplots show median, lower, and upper quartiles (box) and 1.5 times the interquartile range (whiskers). Each circle represents a single patient. Statistical significance highlighted in red (cell counts: t test with robust standard errors on estimated marginal means from linear regression, adjusted for age and sex, $p < 0.05$; cytokine concentrations: t test with robust standard errors on estimated marginal means from tobit regression, adjusted for age and sex, $p < 0.05$). See also Figure S4.

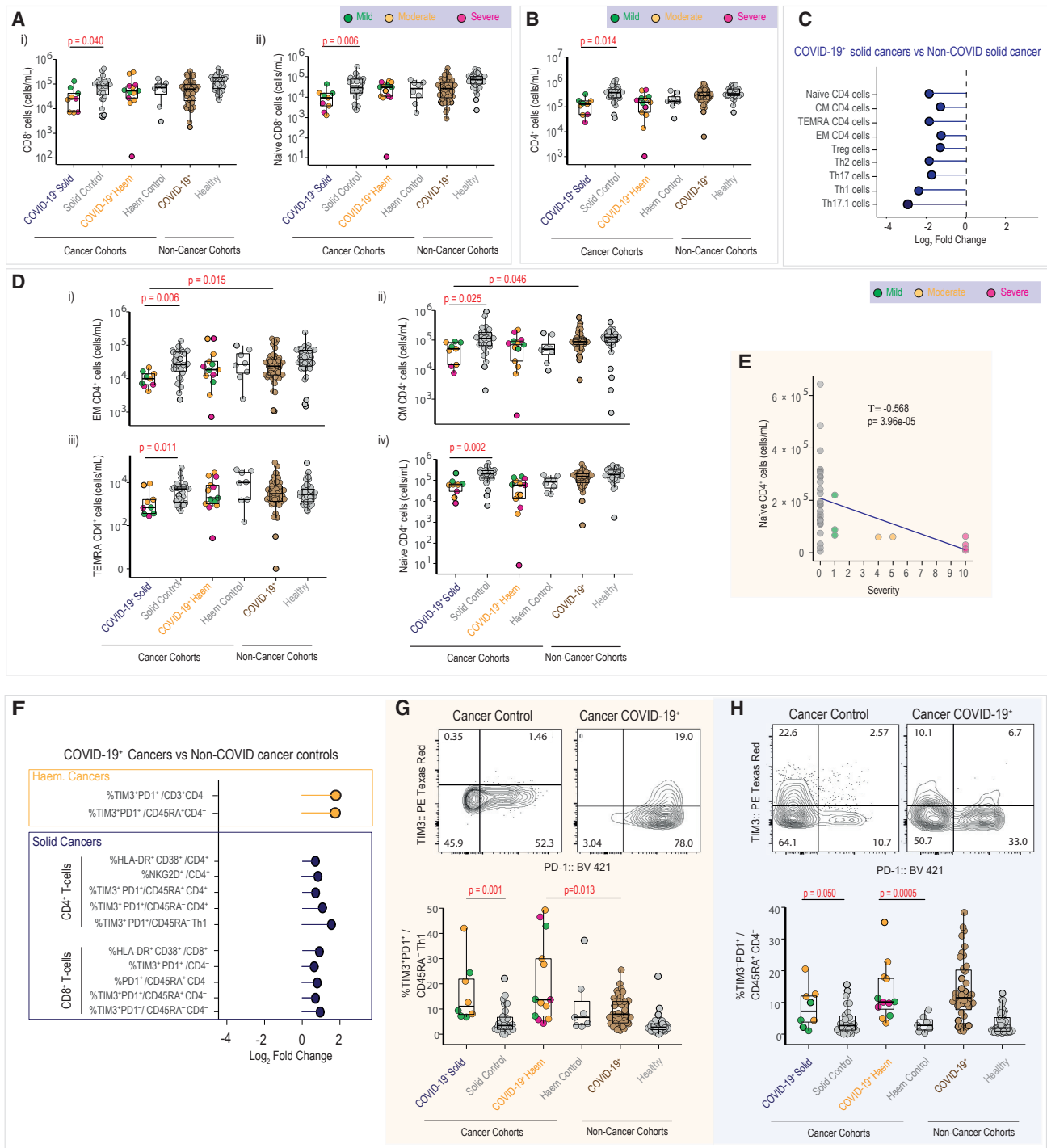


Figure 5. T cell dysfunction in active SARS-CoV-2-infected cancer patients

(A and B) Quantification (cell count/mL) of whole blood (A) (i) CD8 T cells, (ii) naive CD8 T cells, and (B) CD4 T cells.

(C) Log₂ fold change in total counts of major CD4 T cell subpopulations in active COVID-19⁺ solid cancer patients relative to solid cancer non-COVID-19 patients.

(D) Quantified cell counts (cell/mL) of differentiated CD4⁺ T cell (i–iii) and (iv) naive subtypes.

(E) Correlation between naive CD4 T cells and COVID-19 severity in solid cancer patients with active COVID-19 infection (Kendall's tau for semi-partial correlation, adjusted for age and sex, threshold $p < 0.01$).

(F) Log₂ fold change in the frequencies of activation and exhaustion surface marker expression on CD4⁺ and CD8⁺ T cell in solid cancer (dark blue) and hematological cancer (yellow) COVID-19⁺ patients relative to non-COVID-19 cancer patients.

(legend continued on next page)

COVID-19⁺ and non-exposed cancer cohorts were well balanced for tumor type, stage, and treatment. We were able to discern immunological signatures across cancer patients that were most obviously associated with COVID-19 rather than any confounding variables. We demonstrate that the COVID-19 signature for solid cancer patients was a consensus phenotype with striking similarities to the COVID-19 signature of infected subjects without cancer. Some properties were exaggerated in COVID-19⁺ solid cancer patients, but the majority of patients cleared the virus, recovered from COVID-19, and reestablished immunological *status quo*, including several severely ill stage IV cancer patients.

We provide initial evidence of sustained seroconversion in solid cancer patients, providing some measure of confidence that cancer patients are not necessarily at a higher risk of an inferior immune response to SARS-CoV-2 than the general population. Our observations, combined with the large registry studies, suggest that the principal cause of elevated mortality risk from COVID-19 in solid cancer patients is cancer progression (Kuderer et al., 2020), which we show to correlate with the severity of COVID-19. Given recovered solid cancer patients showed no major immunological legacy, we consider that inferior COVID-19-associated cancer outcomes most likely reflect pandemic public health measures preventing optimal cancer care.

In contrast, immune dysregulation in COVID-19⁺ hematological cancer patients showed interindividual variation but collectively was less in the “active” phase, dysregulation increased over time, with particularly striking expression of exhaustion markers by CD8⁺ T cells. In chronic infection, T cell exhaustion manifests as progressive and hierarchical loss of effector function with sustained upregulation and co-expression of multiple inhibitory receptors, including Tim3 and PD1 (Gallimore et al., 1998; McLane et al., 2019; Zajac et al., 1998). Exhausted T cells may compromise virus clearance, consistent with the observation that >70% of COVID-19⁺ hematological cancer patients studied displayed prolonged viral persistence. Failure of virus elimination, and sustained levels of viral antigen may further exacerbate T cell exhaustion. Potentially compounding this, we found significantly increased CD56^{bright} NK cell in the “recovered” hematological COVID-19⁺ cancer patients, suggesting NK cell subsets may be skewed toward inflammation versus cytotoxicity, limiting capacity to control viral infections (Welsh and Waggoner, 2013).

B cell cytopenia was particularly significant in COVID-19⁺ hematological cancer patients. Although anti-CD20 mab is well recognized to deplete CD20⁺ B cells, the COVID-19⁺ and non-COVID-19 hematological cancer cohorts were well matched for underlying malignancies and treatments, suggesting that the exaggerated B cytopenia reflected an increased, albeit indirect vulnerability of malignant B cells to SARS-CoV-2 exposure (Guilpain et al., 2020).

Seroconversion rates 15 days after documented SARS-CoV-2 on rRT-PCR are significantly lower in cancer patients compared

with controls (Solodky et al., 2020). We report longer follow-up of up to 80 days following infection. While most solid cancer patients demonstrated sustained seroconversion, hematological cancer humoral responses were heterogeneous. This may reflect the underlying malignancy and/or treatments such as anti-CD20 mab therapy (Cooper and Arnold, 2010). It is reported that rituximab treatment can be associated with inadequate antibody responses depending on the viral insult (Horwitz et al., 2004; Oren et al., 2008; Villa et al., 2013). Many patients (albeit not all) who failed to mount an antibody response with prolonged viral shedding had received anti-CD20 mab within 4 weeks prior to their first positive swab. These findings may explain conflicting clinical observations over the impact of anti-CD20 therapy on COVID-19⁺ patients (Gianfrancesco et al., 2020). Our data support caution in the use of anti-CD20 mab in chronic lymphocytic leukemia (Rossi et al., 2000) or in indolent lymphomas, especially in those situations where the risk benefit ratio is already established as only marginal. Where such treatments are essential to ensure optimal treatment, patient management should accommodate the potential for prolonged virus infection and transmission.

Failure to clear the virus despite seroconversion in some COVID-19⁺ hematological cohorts indicates that seroconversion alone is insufficient, and that T cell help may be required. Indeed, one patient who had received significant immunosuppression and was post allogeneic bone marrow transplantation demonstrated significant T and B lymphopenia, an inability to clear virus, and was the only patient within the hematological group to succumb to COVID-19.

Finally, a striking feature of SARS-CoV-2 is the exceptional breadth of symptoms it causes. Approximately 25% of the COVID-19⁺ cancer patient population in this study had no symptoms from SARS-CoV-2, providing an opportunity to assess their immune status. Although their overall immune signature was indistinguishable by PCA from those overtly affected, T cell depletion was less severe, and innate cell depletion was more heterogeneous. This validates subset-specific T cytopenia as a marker of severity with prognostic potential, irrespective of underlying cancer.

Risk of transmission remains unclear in COVID-19, with prolonged virus detection especially in asymptomatic carriers being a major concern. Prolonged viral shedding has previously been demonstrated in immunocompromised patients (de Lima et al., 2014; Shah et al., 2020) and recent case reports of such patients with SARS-CoV-2 indicate that this can represent continued infectious virus (Avanzato et al., 2020; Choi et al., 2020). Our results demonstrate high prevalence of prolonged positivity on rRT-PCR swab test among cancer patients in general. The implications of prolonged contagious period for public health measures in the cancer population are profound. For example, it may inform decision making on the isolation of high-risk groups, the role of widespread testing among cancer patients and

(G and H) Representative flow cytometry plots and frequency analysis of (G) PD-1⁺TIM3⁺/CD45RA⁺ Th1 cell and (H) PD-1⁺TIM3⁺/CD45RA⁺CD4⁺ cell. Boxplots show the median, lower and upper quartiles (box), and 1.5 times the interquartile range (whiskers). Each circle represents a single patient. Statistical significance highlighted in red (cell counts: t test with robust standard errors on estimated marginal means from linear regression, adjusted for age and sex, $p < 0.05$; frequencies: Wald test with robust standard errors on estimated marginal means from beta regression, adjusted for age and sex, $p < 0.05$). See also Figure S5.

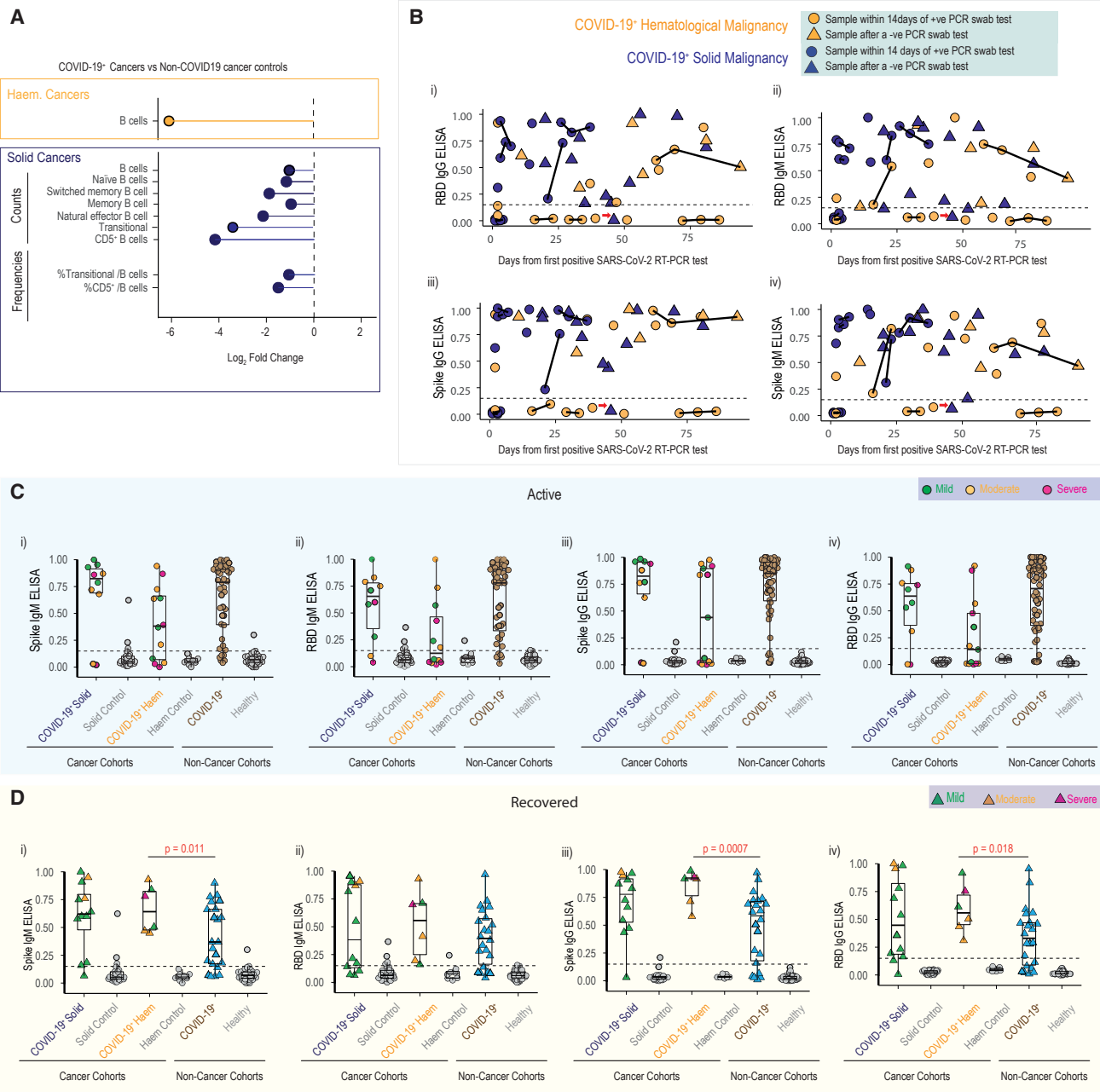


Figure 6. Heterogeneous humoral responses to SARS-CoV-2 in cancer patients

(A) Log₂ fold changes of B cell subtype frequencies and total counts in active COVID-19⁺ infections in solid (dark blue) and hematological (yellow) cancer patients, relative to their respective cancer non-COVID-19 controls.

(B) Antibody titers of COVID-19⁺ cancer patients versus time since first positive rRT-PCR test. Titer measurements for (i) IgG RBD, (ii) IgM RBD, (iii) IgG spike, (iv) IgM spike. Each point represents a single sample, with the status of COVID-19 infection denoted as active (circle) or recovered (triangle) in solid (dark blue) and hematological cancer (yellow) patients. Longitudinal samples from the same patient are linked. Dotted horizontal line indicates the cutoff for sero-positivity (>0.15).

(C and D) Peak antibody titers of IgG and IgM against SARS-CoV-2 spike and RBD in solid, hematological and non-cancer COVID-19⁺ patients, who are either (C) actively infected or (D) recovered. Boxplots show the median, lower and upper quartiles (box), and 1.5 times the interquartile range (whiskers). Shape denotes disease status, active infection (circle), and recovered (triangle). Statistical significance highlighted in red (cell counts: t test with robust standard errors on estimated marginal means from linear regression, adjusted for age and sex, $p < 0.05$; frequencies and serology: Wald test with robust standard errors on estimated marginal means from beta regression, adjusted for age and sex, $p < 0.05$).

See also [Figure S6](#) and [Table S4](#).

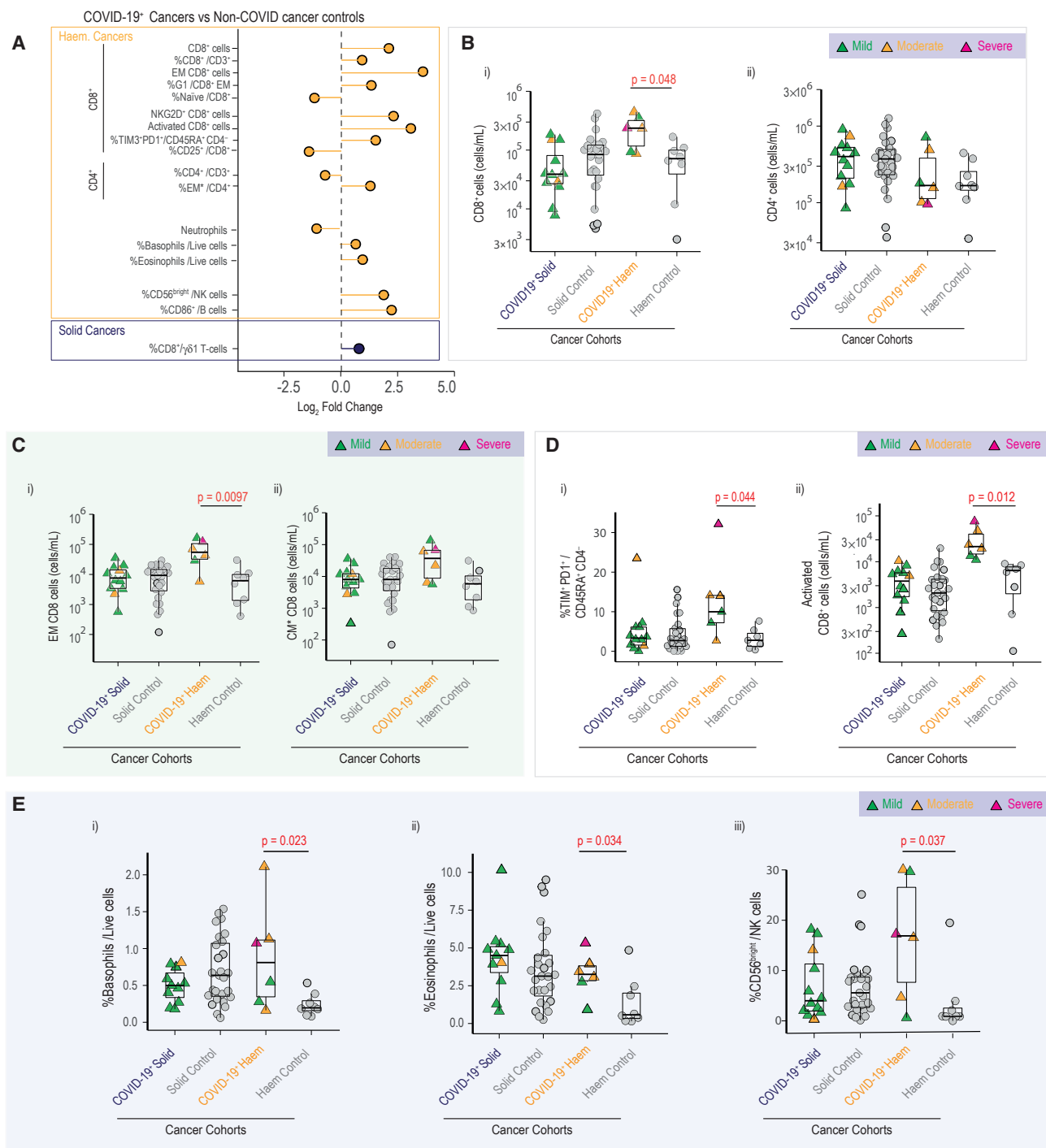


Figure 7. Immune legacies in recovered COVID-19⁺ hematological cancer patients

(A) Log₂ fold changes in frequency and total counts of innate and adaptive immune parameters in recovered COVID-19 solid (dark blue) and hematological (yellow) cancer patients, relative to their respective cancer non-COVID-19 patients.

(B and C) Quantified cell counts of B (i) CD8⁺ and (ii) CD4⁺ T cells; and differentiated CD8⁺ C (i) EM and (ii) CM T cells in whole blood.

(D) (i) Frequency of exhausted T cells via the double positive expression of TIM3⁺PD1⁺ in CD45RA⁺CD4⁺ T cells and (ii) quantified cell count of activated CD8 T cell in whole blood.

(E) Changes in the composition of granulocytic cells, presented through the frequencies of (i) Basophils, (ii) Eosinophils, and (iii) CD56^{bright} NK cells. Boxplots show the median, lower and upper quartiles (box), and 1.5 times the interquartile range (whiskers). Each point represents a single patient. Statistical significance,

(legend continued on next page)

clinical decision making on which patients can safely continue or re-start anti-cancer therapies.

In sum, our data provide reassurance that the immunological status of solid cancer patients does not necessarily put them at a higher risk of an inferior immune response to SARS-CoV-2. This is evidently not the case for a subset of patients with hematological malignancies. While immunological health should be only one factor in determining how to manage a cancer patient in the context of an ongoing pandemic, our findings of delayed or negligible seroconversion, prolonged shedding, and sustained immune dysregulation highlight the need for careful oversight especially of hematological cancer patients. Such issues may be particularly important when considering vaccination, boosting, and follow-up.

Limitations

There are limitations to this study. It was underpowered to detect change for some groups, including the differing treatment modalities, which collectively have differing impacts on host immune compromise. Patients on chemotherapy versus targeted therapies are likely to be the most severely immunocompromised. An important question that remains unanswered is if a “reinforced” immune system following immunotherapy results in an under-/over-activation of the immune response against SARS-CoV-2. Albeit anecdotally, our study cohort included only one such patient who went on to a good outcome. Another limitation is that many of the recruited COVID-19+ cancer patients required prolonged home isolation, during which time it was not feasible to capture longitudinal data through serial blood sampling. Large collaborative efforts are required to overcome the issue of small sample sizes in which regard we hope that others may adopt our readily transferrable experimental analytical SOPs, and benefit from our uploading of data to an open-access portal www.immunophenotype.org.

STAR★METHODS

Detailed methods are provided in the online version of this paper and include the following:

- **KEY RESOURCES TABLE**
- **RESOURCE AVAILABILITY**
 - Lead contact
 - Material availability
 - Data and code availability
- **EXPERIMENTAL MODEL AND SUBJECT DETAILS**
 - Study design and recruitment
- **METHOD DETAILS**
 - Sample processing and staining
 - Data acquisition and processing
 - Patient grouping
- **QUANTIFICATION AND STATISTICAL ANALYSIS**
 - Clinical data correlation and multivariate regression analysis

- High dimensional data analysis of flow cytometry data
- Longitudinal blood parameters
- Correlations with severity
- Principal component analysis

SUPPLEMENTAL INFORMATION

Supplemental Information can be found online at <https://doi.org/10.1016/j.ccell.2021.01.001>.

ACKNOWLEDGMENTS

M. Joseph, D. Davies, J. Freedman, L. Martinez, B. Merrick, K. Bisnauthsing, J. Cason, C. Mant, F. Rosa, J. Edgeworth, and M. Shankar-Hari contributed to the COVID-IP project.

We thank members of the GSTT and KCH trial teams who contributed to patient recruitment for the SOAP study at Guy’s and KCH hospitals; and clinical colleagues at GSTT, KCH, and PRUH for assisting with patient identification and sample collection. The SOAP study (IRAS 282337) is sponsored by King’s College London and Guy’s & St Thomas’ Foundation NHS Trust. It is funded from grants from the KCL Charity funds to S.I. (PS10822), MRC to P.E.P. (T005106), Cancer Research UK to S.I. (C56773/A24869), program grants from Breast Cancer Now including S.I. at King’s College London and to the Breast Cancer Now Toby Robin’s Research Center at the Institute of Cancer Research, London; and the Wellcome Trust Investigator Award to A.C.H. (106292/Z/14/Z), the Rosetrees and John Black Charitable Foundation award to A.C.H. (11130) and is supported by the Cancer Research UK Cancer Immunotherapy Accelerator and the UK COVID-Immunology-Consortium (CIC) (C33499/A20265).

AUTHORS CONTRIBUTIONS

Conceptualization S.A.-J., L.B., I.D., A.G.L., T.H., L.M., M.M.-R., S.P., A.C.H., P.E.P., S.I.
Methodology S.A.-J., I.D., A.G., T.H., L.M., M.M.-R., I.Q., D.M., R.D., K.D.
Formal analysis L.B., S.A.-J., T.A., I.D., A.G., T.H., L.M., M.M.-R., A.L., A.A.K., Y.Z., P.B., M.R., A.C.C., S.I.
Investigation S.A.-J., I.D., T.A., A.L., T.H., L.M., M.M.-R., L.M., I.Q., D.M., R.D., J.C., S.R., E.B., R.Y., S.K., M.F., I.Z., P.V., A.J., S.G., K.D., A.A.K., M.R.
Resource T.A., L.M., D.E., K.B., S.H., J.D.N., R.B., Y.L., J.V., M.K.
Data curation S.A.-J., L.B., T.A., I.D., A.L., T.H., A.L., S.K., C.M., B.R., M.V.H.
Visualization L.B., S.A.-J., T.A., S.I.
Writing original draft P.E.P., S.I.
Writing review and editing S.P., A.R., A.C.C., S.N.K., P.F., M.V.H., J.S., T.N., Y.W., D.E., A.A.K., S.A.-J., L.B., T.A., I.D., A.G.L., T.H., M.M.-R., A.C.H., P.E.P., S.I.
Supervision A.C.H., P.E.P., S.I.
Project administration S.A.-J., A.L., T.H., R.D.
Funding acquisition S.I.

DECLARATION OF INTERESTS

The authors declare no competing interests.

Received: September 30, 2020
Revised: December 2, 2020
Accepted: December 30, 2020
Published: February 8, 2021

REFERENCES

Amanat, F., Stadlbauer, D., Strohmaier, S., Nguyen, T.H.O., Chromikova, V., McMahon, M., Jiang, K., Arunkumar, G.A., Jurczynski, D., Polanco, J., et al.

highlighted in red (cell counts: t test with robust standard errors on estimated marginal means from linear regression, adjusted for age and sex, $p < 0.05$; frequencies: Wald test with robust standard errors on estimated marginal means from beta regression, adjusted for age and sex, $p < 0.05$). See also [Figure S7](#).

- (2020). A serological assay to detect SARS-CoV-2 seroconversion in humans. *Nat. Med.* **26**, 1033–1036.
- Avanzato, V.A., Matson, M.J., Seifert, S.N., Pryce, R., Williamson, B.N., Anzick, S.L., Barbian, K., Judson, S.D., Fischer, E.R., Martens, C., et al. (2020). Case study: prolonged infectious SARS-CoV-2 shedding from an asymptomatic immunocompromised individual with cancer. *Cell* **183**, 1901–1912.e9.
- Brouwer, P.J.M., Caniels, T.G., van der Straten, K., Snitselaar, J.L., Aldon, Y., Bangaru, S., Torres, J.L., Okba, N.M.A., Claireaux, M., Kerster, G., et al. (2020). Potent neutralizing antibodies from COVID-19 patients define multiple targets of vulnerability. *Science* **369**, 643–650.
- Choi, B., Choudhary, M.C., Regan, J., Sparks, J.A., Padera, R.F., Qiu, X., Solomon, I.H., Kuo, H.-H., Boucau, J., Bowman, K., et al. (2020). Persistence and evolution of SARS-CoV-2 in an immunocompromised host. *New Engl. J. Med.* **383**, 2291–2293.
- Cooper, N., and Arnold, D.M. (2010). The effect of rituximab on humoral and cell mediated immunity and infection in the treatment of autoimmune diseases. *Br. J. Haematol.* **149**, 3–13.
- Diao, B., Wang, C., Tan, Y., Chen, X., Liu, Y., Ning, L., Chen, L., Li, M., Liu, Y., Wang, G., et al. (2020). Reduction and functional exhaustion of T cells in patients with coronavirus disease 2019 (COVID-19). *Front. Immunol.* **11**, 827.
- Gallimore, A., Glithero, A., Godkin, A., Tissot, A.C., Plücker, A., Elliott, T., Hengartner, H., and Zinkernagel, R. (1998). Induction and exhaustion of lymphocytic choriomeningitis virus-specific cytotoxic T lymphocytes visualized using soluble tetrameric major histocompatibility complex class I-peptide complexes. *J. Exp. Med.* **187**, 1383–1393.
- Gianfrancesco, M., Hyrich, K.L., Al-Adely, S., Carmona, L., Danila, M.I., Gossec, L., Izadi, Z., Jacobsohn, L., Katz, P., Lawson-Tovey, S., et al. (2020). Characteristics associated with hospitalisation for COVID-19 in people with rheumatic disease: data from the COVID-19 Global Rheumatology Alliance physician-reported registry. *Ann. Rheum. Dis.* **79**, 859–866.
- Gralinski, L.E., and Baric, R.S. (2015). Molecular pathology of emerging coronavirus infections. *J. Pathol.* **235**, 185–195.
- Guilpain, P., Le Bihan, C., Foulongne, V., Taourel, P., Pansu, N., Maria, A.T.J., Jung, B., Larcher, R., Klouche, K., and Le Moing, V. (2020). Rituximab for granulomatosis with polyangiitis in the pandemic of covid-19: lessons from a case with severe pneumonia. *Ann. Rheum. Dis.* **80**, e10.
- He, X., Lau, E.H.Y., Wu, P., Deng, X., Wang, J., Hao, X., Lau, Y.C., Wong, J.Y., Guan, Y., Tan, X., et al. (2020). Temporal dynamics in viral shedding and transmissibility of COVID-19. *Nat. Med.* **26**, 672–675, <https://doi.org/10.1038/s41591-020-0869-5>.
- Horwitz, S.M., Negrin, R.S., Blume, K.G., Breslin, S., Stuart, M.J., Stockerl-Goldstein, K.E., Johnston, L.J., Wong, R.M., Shizuru, J.A., and Horning, S.J. (2004). Rituximab as adjuvant to high-dose therapy and autologous hematopoietic cell transplantation for aggressive non-Hodgkin lymphoma. *Blood* **103**, 777–783.
- Huang, C., Wang, Y., Li, X., Ren, L., Zhao, J., Hu, Y., Zhang, L., Fan, G., Xu, J., Gu, X., et al. (2020). Clinical features of patients infected with 2019 novel coronavirus in Wuhan, China. *The Lancet* **395**, 497–506.
- Kim, S. (2015). Ppcor: an R package for a Fast calculation to semi-partial correlation coefficients. *Commun. Stat. Appl. Methods* **22**, 665–674.
- Kuderer, N.M., Choueiri, T.K., Shah, D.P., Shyr, Y., Rubinstein, S.M., Rivera, D.R., Shete, S., Hsu, C.Y., Desai, A., de Lima Lopes, G., Jr., et al. (2020). Clinical impact of COVID-19 on patients with cancer (CCC19): a cohort study. *Lancet* **395**, 1907–1918.
- Laing, A.G., Lorenc, A., Del Molino Del Barrio, I., Das, A., Fish, M., Monin, L., Muñoz-Ruiz, M., McKenzie, D.R., Hayday, T.S., Francos-Quijorna, I., et al. (2020). A dynamic COVID-19 immune signature includes associations with poor prognosis. *Nat. Med.* **26**, 1623–1635.
- Lee, L.Y., Cazier, J.B., Angelis, V., Arnold, R., Bisht, V., Campton, N.A., Chackathayil, J., Cheng, V.W., Curley, H.M., Fittall, M.W., et al. (2020). COVID-19 mortality in patients with cancer on chemotherapy or other anti-cancer treatments: a prospective cohort study. *Lancet* **395**, 1919–1926.
- de Lima, C.R., Mirandola, T.B., Carneiro, L.C., Tusset, C., Romer, C.M., Andreolla, H.F., Baethgen, L.F., and Pasqualotto, A.C. (2014). Prolonged respiratory viral shedding in transplant patients. *Transpl Infect Dis.* **16**, 165–169, <https://doi.org/10.1111/tid.12167>.
- Lucas, C., Wong, P., Klein, J., Castro, T.B.R., Silva, J., Sundaram, M., Ellingson, M.K., Mao, T., Oh, J.E., Israelow, B., et al. (2020). Longitudinal analyses reveal immunological misfiring in severe COVID-19. *Nature* **584**, 463–469.
- Maringe, C., Spicer, J., Morris, M., Purushotham, A., Nolte, E., Sullivan, R., Racht, B., and Aggarwal, A. (2020). The impact of the COVID-19 pandemic on cancer deaths due to delays in diagnosis in England, UK: a national, population-based, modelling study. *Lancet Oncol.* **21**, 1023–1034.
- Marshall, J.C., Murthy, S., Diaz, J., Adhikari, N.K., Angus, D.C., Arabi, Y.M., Baillie, K., Bauer, M., Berry, S., Blackwood, B., et al. (2020). A minimal common outcome measure set for COVID-19 clinical research. *Lancet Infect. Dis.* **20**, e192–e197.
- Mathew, D., Giles, J.R., Baxter, A.E., Oldridge, D.A., Greenplate, A.R., Wu, J.E., Alanio, C., Kuri-Cervantes, L., Pampena, M.B., D’Andrea, K., et al. (2020). Deep immune profiling of COVID-19 patients reveals distinct immunotypes with therapeutic implications. *Science* **369**, eabc8511.
- McLane, L.M., Abdel-Hakeem, M.S., and Wherry, E.J. (2019). CD8 T cell exhaustion during chronic viral infection and cancer. *Annu. Rev. Immunol.* **37**, 457–495.
- Oren, S., Mandelboim, M., Braun-Moscovici, Y., Paran, D., Ablin, J., Litinsky, I., Comaneshter, D., Levartovsky, D., Mendelson, E., Azar, R., et al. (2008). Vaccination against influenza in patients with rheumatoid arthritis: the effect of rituximab on the humoral response. *Ann. Rheum. Dis.* **67**, 937–941.
- Pickering, S., Betancor, G., Galão, R.P., Merrick, B., Signell, A.W., Wilson, H.D., Kia Ik, M.T., Seow, J., Graham, C., Acors, S., et al. (2020). Comparative assessment of multiple COVID-19 serological technologies supports continued evaluation of point-of-care lateral flow assays in hospital and community healthcare settings. *PLoS Pathog.* **16**, e1008817.
- Pinato, D.J., Zambelli, A., Aguilar-Company, J., Bower, M., Sng, C., Salazar, R., Bertuzzi, A., Brunet, J., Mesia, R., Segui, E., et al. (2020). Clinical portrait of the SARS-CoV-2 epidemic in European cancer patients. *Cancer Discov.* **10**, 1465–1474.
- Prompetchara, E., Ketloy, C., and Palaga, T. (2020). Immune responses in COVID-19 and potential vaccines: lessons learned from SARS and MERS epidemic. *Asian Pac. J. Allergy Immunol.* **38**, 1–9.
- Rodriguez, L., Pekkarinen, P.T., Lakshminanth, T., Tan, Z., Consiglio, C.R., Pou, C., Chen, Y., Mugabo, C.H., Nguyen, N.A., Nowlan, K., et al. (2020). Systems-level immunomonitoring from acute to recovery phase of severe COVID-19. *Cell Rep. Med.* **1**, 100078.
- Rossi, D., Shadman, M., Condoluci, A., Brown, J.R., Byrd, J.C., Gaidano, G., Hallek, M., Hillmen, P., Mato, A., Montserrat, E., et al. (2020). How we manage patients with chronic lymphocytic leukemia during the SARS-CoV-2 pandemic. *Hemasphere* **4**, e432, <https://doi.org/10.1097/HS9.0000000000000432>.
- Russell, B., Moss, C., George, G., Santaolalla, A., Cope, A., Papa, S., and Van Hemelrijck, M. (2020a). Associations between immune-suppressive and stimulating drugs and novel COVID-19: a systematic review of current evidence. *Ecancermedicinescience* **14**, 1022.
- Russell, B., Moss, C., Papa, S., Irshad, S., Ross, P., Spicer, J., Kordasti, S., Crawley, D., Wylie, H., Cahill, F., et al. (2020b). Factors affecting COVID-19 outcomes in cancer patients: a first report from guy’s cancer center in London. *Front. Oncol.* **10**, 1279.
- Sekine, T., Perez-Potti, A., Rivera-Ballesteros, O., Strålin, K., Gorin, J.-B., Olsson, A., Llewellyn-Lacey, S., Kamal, H., Bogdanovic, G., Muschiol, S., et al. (2020a). Robust T cell immunity in convalescent individuals with asymptomatic or mild COVID-19. *Cell* **183**, 158–168.e114.
- Sekine, T., Perez-Potti, A., Rivera-Ballesteros, O., Strålin, K., Gorin, J.-B., Olsson, A., Llewellyn-Lacey, S., Kamal, H., Bogdanovic, G., Muschiol, S., et al. (2020b). Robust T cell immunity in convalescent individuals with asymptomatic or mild COVID-19. *Cell* **183**, 158–168.e14.

- Seow, J., Graham, C., Merrick, B., Acors, S., Pickering, S., Steel, K.J.A., Hemmings, O., O'Byrne, A., Kouphou, N., Galao, R.P., et al. (2020). Longitudinal observation and decline of neutralizing antibody responses in the three months following SARS-CoV-2 infection in humans. *Nat. Microbiol.* *5*, 1598–1607.
- Shah, V., Ko Ko, T., Zuckerman, M., Vidler, J., Sharif, S., Mehra, V., Gandhi, S., Kuhl, A., Yallop, D., Avenoso, D., et al. (2020). Poor outcome and prolonged persistence of SARS-CoV-2 RNA in COVID-19 patients with haematological malignancies; King's College Hospital experience. *Br. J. Haematol.* *190*, e279–e282.
- Solodky, M.L., Galvez, C., Russias, B., Detourbet, P., N'Guyen-Bonin, V., Herr, A.L., Zrounba, P., and Blay, J.Y. (2020). Lower detection rates of SARS-COV2 antibodies in cancer patients versus health care workers after symptomatic COVID-19. *Ann. Oncol.* *31*, 1087–1088.
- Ueda, M., Martins, R., Hendrie, P.C., McDonnell, T., Crews, J.R., Wong, T.L., McCreery, B., Jagels, B., Crane, A., Byrd, D.R., et al. (2020). Managing cancer care during the COVID-19 pandemic: agility and collaboration toward a common goal. *J. Natl. Compr. Canc. Netw.* *18*, 366.
- Uh, H.-W., Hartgers, F.C., Yazdanbakhsh, M., and Houwing-Duistermaat, J.J. (2008). Evaluation of regression methods when immunological measurements are constrained by detection limits. *BMC Immunol.* *9*, 59.
- Vijenthira, A., Gong, I.Y., Fox, T.A., Booth, S., Cook, G., Fattizzo, B., Martin Moro, F., Razanamahery, J., Riches, J.C., Zwicker, J.I., et al. (2020). Outcomes of patients with hematologic malignancies and COVID-19: a systematic review and meta-analysis of 3377 patients. *Blood* *136*, 2881–2892.
- Villa, D., Gubbay, J., Sutherland, D.R., Laister, R., McGeer, A., Cooper, C., Fortuno, E.S., 3rd, Xu, W., Shi, L., Kukreti, V., et al. (2013). Evaluation of 2009 pandemic H1N1 influenza vaccination in adults with lymphoid malignancies receiving chemotherapy or following autologous stem cell transplant. *Leuk. Lymphoma* *54*, 1387–1395.
- Welsh, R.M., and Waggoner, S.N. (2013). NK cells controlling virus-specific T cells: rheostats for acute vs. persistent infections. *Virology* *435*, 37–45.
- Wen, W., Su, W., Tang, H., Le, W., Zhang, X., Zheng, Y., Liu, X., Xie, L., Li, J., Ye, J., et al. (2020). Immune cell profiling of COVID-19 patients in the recovery stage by single-cell sequencing. *Cell Discov.* *6*, 31.
- Williamson, E.J., Walker, A.J., Bhaskaran, K., Bacon, S., Bates, C., Morton, C.E., Curtis, H.J., Mehrkar, A., Evans, D., Inglesby, P., et al. (2020). Factors associated with COVID-19-related death using OpenSAFELY. *Nature* *584*, 430–436.
- Xu, Z., Shi, L., Wang, Y., Zhang, J., Huang, L., Zhang, C., Liu, S., Zhao, P., Liu, H., Zhu, L., et al. (2020). Pathological findings of COVID-19 associated with acute respiratory distress syndrome. *Lancet Respir. Med.* *8*, 420–422.
- Yang, Y., Shen, C., Li, J., Yuan, J., Wei, J., Huang, F., Wang, F., Li, G., Li, Y., Xing, L., et al. (2020). Plasma IP-10 and MCP-3 levels are highly associated with disease severity and predict the progression of COVID-19. *J. Allergy Clin. Immunol.* *146*, 119–127, e114.
- Young, B.E., Ong, S.W.X., Kalimuddin, S., Low, J.G., Tan, S.Y., Loh, J., Ng, O.T., Marimuthu, K., Ang, L.W., Mak, T.M., et al. (2020). Epidemiologic features and clinical course of patients infected with SARS-CoV-2 in Singapore. *JAMA* *323*, 1488–1494, <https://doi.org/10.1001/jama.2020.3204>.
- Zajac, A.J., Blattman, J.N., Murali-Krishna, K., Sourdive, D.J., Suresh, M., Altman, J.D., and Ahmed, R. (1998). Viral immune evasion due to persistence of activated T cells without effector function. *J. Exp. Med.* *188*, 2205–2213.

STAR★METHODS

KEY RESOURCES TABLE

REAGENT or RESOURCE	SOURCE	IDENTIFIER
Antibodies		
CD3 FITC (Clone UCHT1)	BD	Cat#: 555332; RRID: AB_395739
CD3 APC-Cy7 (Clone OKT3)	Biolegend	Cat#: 317342; RRID: AB_2563410
CD3 BUV395 (Clone UCHT1)	BD	Cat#: 563546; RRID: AB_2744387
CD4 BV711 (Clone SK3)	BD	Cat#: 563028; RRID: AB_2737961
CD4 PE-Cy7 (Clone SK3)	BD	Cat#: 557852; RRID: AB_396897
CD4 BV510 (Clone SK3)	BD	Cat#: 562970; RRID: AB_2744424
CD8 PerCp-Cy5.5 (Clone SK1)	BD	Cat#: 565310; RRID: AB_2687497
CD8 FITC (Clone SK1)	BD	Cat#: 345772; RRID: AB_2868800
CD25 APC-R700 (Clone 2A3)	BD	Cat#: 565106; RRID: AB_2744339
CD25 PE (Clone 2A3)	BD	Cat#: 341011; RRID: AB_2783790
CD25 PE (Clone M-A251)	BD	Cat#: 555432; RRID: AB_395826
CD127 BV786 (Clone HIL-7R-M21)	BD	Cat#: 563324; RRID: AB_2738138
CD103 BV711 (Clone BER-ACT08)	BD	Cat#: 563162; RRID: AB_2738039
CD103 BV421 (Clone Ber-ACT8)	BD	Cat#: 563882; RRID: AB_2738464
CD27 BV786 (Clone L128)	BD	Cat#: 563327; RRID: AB_2744353
CD27 BV605 (Clone L128)	BD	Cat#: 562655; RRID: AB_2744351
CD45 PerCP (Clone HI30)	Biolegend	Cat#: 304026; RRID: AB_893337
CD45 AF700 (Clone HI30)	BD	Cat#: 560566; RRID: AB_1645452
CD45RA BV786 (Clone HI100)	BD	Cat#: 563870; RRID: AB_2738459
CD45RA PE-Cy7 (Clone HI100)	BD	Cat#: 560675; RRID: AB_1727498
CD19 BV711 (Clone SJ25C1)	BD	Cat#: 563036; RRID: AB_2737968
CD19 PE (Clone HIB19)	Biolegend	Cat#: 302208; RRID: AB_314238
CD19 BUV737 (Clone SJ25C1)	BD	Cat#: 612756; RRID: AB_2870087
CD14 AF488 (Clone HCD14)	Biolegend	Cat#: 325610; RRID: AB_830683
CD14 BV711 (Clone MφP9)	BD	Cat#: 563372; RRID: AB_2744290
CD15 BV605 (Clone W6D3)	Biolegend	Cat#: 323032; RRID: AB_2562132
CD56 APC (Clone HCD56)	Biolegend	Cat#: 318310; RRID: AB_604106
CD56 PE-CF594 (Clone NCAM16.2)	BD	Cat#: 564849; RRID: AB_2738983
CD16 PE-Cy7 (Clone 3G8)	Biolegend	Cat#: 302016; RRID: AB_314216
CD16 PerCp-Cy5.5 (Clone 3G8)	BD	Cat#: 560717; RRID: AB_1727434
NKG2D APC (Clone 1D11)	BD	Cat#: 558071; RRID: AB_398654
CCR4 AF647 (Clone 1G1)	BD	Cat#: 557863; RRID: AB_396906
CCR6 BB515 (Clone 11A9)	BD	Cat#: 564479; RRID: AB_2738825
CCR6 BV421 (Clone 11A9)	BD	Cat#: 562515; RRID: AB_11154229
CCR7 PE-CF594 (Clone 150503)	BD	Cat#: 562381; RRID: AB_11153301
HLA-DR BV510 (Clone G46-6)	BD	Cat#: 563083; RRID: AB_2737994
HLA-DR PerCp-Cy5.5 (Clone L243)	BD	Cat#: 339216; RRID: AB_2868719
CXCR3 BB700 (Clone CXCR3-173)	BD	Cat#: 742274; RRID: AB_2871450
CXCR3 PE-Cy5 (Clone 1C6)	BD	Cat#: 551128; RRID: AB_394061
CD38 PE (Clone HIT-2)	BD	Cat#: 555460; RRID: AB_395853
CD38 BUV737 (Clone HB7)	BD	Cat#: 612824; RRID: AB_2870148
TCR PAN $\gamma\delta$ PE-Cy7 (Clone IMMU510)	Beckman Coulter	Cat#: B10247
V δ 1 FITC (Clone REA173)	Miltenyi	Cat#: 130-118-362; RRID: AB_2751495

(Continued on next page)

Continued

REAGENT or RESOURCE	SOURCE	IDENTIFIER
V δ 2 PE (Clone B6)	BD	Cat#: 555739; RRID: AB_396082
PD-1 BV421 (Clone EH12.1)	BD	Cat#: 562516; RRID: AB_11153482
IgD BUV737 (Clone IA6-2)	BD	Cat#: 612798; RRID: AB_2870125
IgM BB515 (Clone G20-127)	BD	Cat#: 564622; RRID: AB_2738869
IgG APC (Clone G18-145)	BD	Cat#: 550931; RRID: AB_398478
CD43 BV421 (Clone 1610)	BD	Cat#: 562916; RRID: AB_2737890
CD24 BUV395 (Clone ML5)	BD	Cat#: 563818; RRID: AB_2632389
CD5 PE-Cy7 (Clone L17F12)	BD	Cat#: 348810; RRID: AB_2848145
FOXP3 AF647 (Clone 259D)	Biologend	Cat#: 320214; RRID: AB_492984
Ki67 AF700 (Clone B56)	BD	Cat#: 561277; RRID: AB_10611571
LAG-3 BV510 (Clone TA7-530)	BD	Cat#: 744985; RRID: AB_2742625
TIM3 PE-CF594 (Clone 7D3)	BD	Cat#: 565560; RRID: AB_2744371
2B4 APC (Clone 2-69)	BD	Cat#: 562350; RRID: AB_11153502
CD64 BV421 (Clone 10.1)	Biologend	Cat#: 305020; RRID: AB_2561828
CD62L BV785 (Clone DREG-56)	Biologend	Cat#: 304830; RRID: AB_2629555
CD10 BV711 (Clone HI10a)	Biologend	Cat#: 312226; RRID: AB_2565876
Goat-anti-human IgM-HRP	Sigma	Cat#: A6097; RRID: AB_258318
Goat-anti-human-Fc-AP	Jackson	Cat#: 109-055-098; RRID: AB_2337608

Biological Samples

Peripheral Blood samples from Cancer COVID-19+/- patients	Guy's and St Thomas' Trust Hospitals. King's College Hospital. Princess Royal University Hospital	IRAS ID: 282337 REC ID: 20/HRA/2031
Peripheral Blood samples from COVID-19+	Guy's and St Thomas' Trust Hospitals	Laing et al., 2020
Peripheral Blood samples from healthy volunteers	Guy's and St Thomas' Trust Hospitals	Laing et al., 2020

Chemicals, Peptides, and Recombinant Proteins

N protein SARS-CoV-2 (residues 48-365)	L. James and J. Luptak at LMB, Cambridge	Seow et al., 2020
S glycoprotein ectodomain (residues 1-1138) with GGGG substitution at the furin cleavage site (aa 682-685), proline substitutions at aa 986 and 987	P. Brouwer, M. van Gils and R. Sanders at the University of Amsterdam	Brouwer et al., 2020
RBD protein SARS-CoV-2 (residues 319-541)	F. Krammer at Mount Sinai University	Amanat et al., 2020

Critical Commercial Assays

LegendPlex Human Anti-Virus Response panel (13-plex)	Biologend	Cat#: 740390; RRID: AB_2740120
LegendPlex Human Th Panel (13-plex)	Biologend	Cat#: 740721; RRID: AB_10697752

Deposited Data

RAW dataset: Flowcytometry, serology and cytokine (megatable)	This paper	https://www.immunophenotype.org
Code depository – Statistical analysis	This paper	https://github.com/irshadgroup/SOAP

Software and Algorithms

R 4.0.0	R Core Team	https://www.R-project.org/
AER 1.2.9	Kleiber C, Zeileis A (2008), ISBN 978-0-387-77316-2	https://CRAN.R-project.org/package=AER
betareg 3.1.3	Bettina Gruen, Ioannis Kosmidis, Achim Zeileis (2012), http://www.jstatsoft.org/v48/i11/	https://CRAN.R-project.org/package=betareg
emmeans 1.4.8	Lenth R (2020)	https://CRAN.R-project.org/package=emmeans

(Continued on next page)

Continued

REAGENT or RESOURCE	SOURCE	IDENTIFIER
sandwich 2.5.1	Zeileis A (2006), https://doi.org/10.18637/jss.v016.i09	https://CRAN.R-project.org/package=sandwich
qvalue 2.21.0	Storey JD, Bass AJ, Dabney A, Robinson D (2020)	http://github.com/jdstorey/qvalue
ppcor 1.1	Seongho Kim (2015)	https://CRAN.R-project.org/package=ppcor
SaddlePoint-Signature version 2.9.3.	SaddlePoint Science	https://www.saddlepointscience.com/products.html
FACSDIVA v.8	BD Bioscience	RRID:SCR_001456
LegendPlex™ Data Analysis V8 for PC	Biolegend	https://www.biolegend.com/en-gb/legendplex
FlowJo v 10.6.2	BD Bioscience	RRID:SCR_008520
Prism v8.4.3	Graphpad Software	RRID:SCR_002798

RESOURCE AVAILABILITY

Lead contact

Further information and requests for resources and reagents should be directed to and will be fulfilled by the Lead Contact, Sheeba Irshad (sheeba.irshad@kcl.ac.uk).

Material availability

This study did not generate new unique reagents.

Data and code availability

The complete dataset generated in this study, including the serology, cytokine and flow cytometry analysis of cell counts and frequency data has been collated into a megatable and will be available on <https://www.immunophenotype.org>.

Scripts used for data analysis will be available via <https://github.com/irshadgroup/SOAP>.

EXPERIMENTAL MODEL AND SUBJECT DETAILS

Study design and recruitment

Patients with a known diagnosis of cancer presenting at Guy's and St Thomas' Trust Hospitals, King's College Hospital or Princess Royal University Hospital with a confirmed positive SARS-CoV-2 rRT-PCR test were screened and approached for informed consent into the SOAP study (IRAS ID: 282337 REC ID: 20/HRA/2031). Peripheral blood was collected from all subjects. Where possible, temporal blood sampling over the course of the patient's symptoms were taken, spaced out at least 2-4 days apart. Cancer patients with no recent symptoms consistent with COVID-19 and a confirmed negative SARS-CoV-2 rRT-PCR test were recruited as a control cohort for similar serial peripheral blood immunophenotyping. The control cancer patients were approached according to four matching criteria (age, tumour type, tumour stage and last treatment modality). Associated clinical data were abstracted from hospital specific software systems and medical notes into standardized case report forms (Russell et al., 2020b). Clinical laboratory data at the time of worst symptoms or disease severity were extracted for analysis. The World Health Organisation (WHO) clinical progression scale was employed to provide a measure of illness severity across a range from 0 (not infected) to 10 (deceased) with data elements that were rapidly obtainable from clinical records (Figure 1A) (Marshall et al., 2020). All data was handled in accordance with the Data Protection Act 2018 and General Data Protection Guidance (2018). All participants provided informed consent in accordance with protocols approved by the regional ethical research boards and the Declaration of Helsinki.

METHOD DETAILS

The SOAP and Covid-ImmunoPhenotyping (COVID-IP) studies were done together simultaneously, using a single pipeline over the duration of the study (Laing et al., 2020).. Samples for both studies were collected daily, processed and analysed using the same materials, standard-operating-protocols and personnel.

Sample processing and staining

Fresh whole blood samples were collected in either heparin (BD Biosciences, Franklin Lakes, NJ, and USA) or serum separating tubes as indicated for specific experiments. Sample processing was performed under Biosafety Level 3 containment conditions

and prior to removal from the facility, flow samples were fixed for 10 min with either Cellfix (BD) or FoxP3 Fix/Perm kit (eBioscience). Details of staining mix antibodies and concentrations for panels 1-8 can be found in [Table S5](#).

Whole blood staining: 50 μ l of whole blood from heparinised tubes was stained in 50 μ l of antibody staining mix (panels 6-8; [Table S5](#)). Cell surface staining was performed in BD Pharmingen™ Stain Buffer (BSA) and BD Horizon™ Brilliant Stain Buffer Plus for 20min at RT, washed in DPBS and fixed for 10 min with Cellfix (BD). This was followed by two rounds of red blood cell lysis using eBioscience RBC Lysis Buffer (Multi-species) 10X diluted in deionized water (RT, 15min) then resuspended in 200ml staining buffer for flow cytometry.

PBMC staining: Remaining whole blood was diluted with PBS 1:1 and processed to extract the PBMC fraction using Ficoll gradient. The PBMC fraction was then washed three times in cold PBS and used for flow cytometry. PBMCs were stained with BD Horizon™ Fixable Viability Stain 780 (live/dead mix). Cell surface staining was performed using BD Pharmingen™ Stain Buffer (BSA) and BD Horizon™ Brilliant Stain Buffer Plus (RT, 30min). For intracellular staining, cells were permeabilised using Invitrogen Permeabilization Buffer 10X (4°C, 30 min). PBMC samples were stained in 100ml staining mix (Panels 1-5), washed in staining buffer prior to an hour fixation in the dark, and followed by another wash and resuspension in 200 μ l staining buffer for acquisition for panels 1-4. As for panel 5, after fixation PBMCs were resuspended in permeabilization buffer containing intracellular staining antibodies, then washed with DPBS and resuspended in DPBS containing Hoechst 33342 (ThermoFisher Scientific) (RT, 15min) before a final wash and resuspension in 200ml DPBS for acquisition.

Cytokine profiling: Aliquots of whole blood from heparin tubes were centrifuged at 2000 x g for 10 min and plasma stored at -80°C. Cytokine levels in from thawed plasma were analysed using LegendPlex assay panels, Human Anti-Virus Response panel (740390, Biolegend) and Human Th Panel (740721, Biolegend) with some modifications to the manufacturer's instructions. The panel included: IL-1 β , IL-6, IL-8, IL-10, IL-12p70, IFN- α 2, IFN- β , IFN- λ 1, IFN- λ 2/3, IFN- γ , TNF- α , IP-10, GM-CSF, IL-15, IL-13, IL-2, IL-9, IL-17A, IL-17F, IL-4, IL-21, IL-22. Plasma and all reagents were diluted 2-fold in assay buffer, with 25 μ l of each reagent used in the assay in a 96-well V-bottom plate. Samples and standards were first incubated with mixed beads for 90 min, followed by two washes, a 45 min incubation with detection antibodies with Streptavidin-PE added on thereafter for 20 min, before a final wash and resuspension in 200 μ l wash buffer for acquisition (BD LSR Fortessa X20). Incubation steps were at RT, in the dark on orbital shaker set at 600rpm. LegendPlex data analysis software Version 8 for windows was used for data analysis.

Serology Analysis by ELISA: Three SARS-CoV-2 proteins were used for serology analysis; (1) Nucleocapsid (N) protein, obtained from Leo James and Jakob Luptak at LMB, Cambridge; (2) Spike (S) protein, plasmid obtained from from Philip Brouwer, Marit van Gils and Rogier Sanders at The University of Amsterdam ([Brouwer et al., 2020](#)); and (3) Receptor binding domain (RBD), plasmid obtained from Florian Krammer at Mount Sinai University ([Amanat et al., 2020](#)). The N protein is a truncated construct comprising residues 48-365 with a uncleavable hexahistidine tag N terminal. It was expressed in E. Coli using autoinducing media for 7h at 37°C and purified using immobilised metal affinity chromatography (IMAC), size exclusion chromatography and heparin chromatography ([Seow et al., 2020](#)). The S protein comprised of residues 1-1138 of the prefusion S ectodomain with a GGGG substitution at amino acids (aa) positions 682-685 in the furin cleavage site, a proline substitutions at aa 986 and 987 and a T4 trimerisation at the N terminal domain followed by a Strep-tag II. Protein expression was achieved in HEK-293F cells (Invitrogen) (1.5 million cells/mL) and transfected with 325 μ g of DNA at a 1:3 ratio using PEI-Max (1 mg/mL, Polysciences). Supernatant was purified using StrepTactinXT Superflow high capacity 50% suspension according to the manufacturer's protocol by gravity flow (IBA Life Sciences) after 7 days of harvesting. The RBD proteins consists of residues 319-541 with a fusion at the start of the sequence of the S protein natural N-terminal signal peptide and joined to C-terminal hexahistidine tag. Protein expression again was achieved in HEK-293F cells at a density of 1.5 million cells/mL transfected with 1000 μ g of DNA using PEI-Max at a ratio of 1:3 with supernatant purified using Ni-NTA agarose beads after 7 days of harvesting. An in-house ELISA was used to detect antibodies in heat-inactivated plasma samples (56°C for 30 mins). High-binding ELISA plates (Corning, 3690) were coated with 3 μ g/mL of antigens (N, S or RBD) in PBS (overnight at 4°C or 2 hr at 37°C), then washed with PBS-T and blocked with 5% milk in PBS-T (RT, 60 min). Plasma was diluted in milk at 1:25 respectively then added onto the plate and incubated at RT for 2h, followed by a wash, next adding the secondary antibody at 1:1000 (RT, 60 min), then a final wash before adding the substrate. Substrates used were either AP substrate (Sigma) read at 405 nm (AP), or 1-step TMB substrate (Thermo Scientific) read at 450 nm (HRP). IgG was detected using Goat-anti-human-Fc-AP (Jackson: 109-055-098 -JIR) and IgM was detected using Goat-anti-human-IgM-HRP (Sigma: A6907). Control reagents were CR3009 (2 μ g/mL), CR3022 (0.2 μ g/mL), negative control plasma (1:25), positive control plasma (1:50) and blank wells. Data were normalized using a min/max normalization to compare samples across batches. Values >0.15 were considered positive, which is 4 fold of background based on results from 300 patient samples pre-COVID-19 ([Pickering et al., 2020](#)) ([Table S4](#)).

Data acquisition and processing

PBMCs stained with panels 1-4 were analysed using a five laser BD LSRFortessa, whilst whole

bloods stained with panels 6-8 were analysed on a 4 laser BD LSRFortessa. For both, 100 μ l of sample was acquired using a BD High Throughput Sampler (HTS). Panel 5 PBMCs were acquired on a 4 laser BD LSRFortessa in FACS tubes, run on low for 10 mins, with samples diluted to achieve an event rate of no more than approximately 200 events/s. FCS files were analysed using FlowJo (10.6.2, Treestar), exporting counts of all gates and calculating frequencies of interest in R. Flow gating strategy for panels 1-8 is illustrated in [Figure S8](#) and key cell definitions are in [Table S6](#). Absolute cell counts were back calculated using the cell/ml of blood of the major lineages from whole blood count panel (panel 6), where the equivalent of 25 μ l of whole blood was analysed per sample.

For panels 1-4, 6-7 we required at least 30 events in a parental population to investigate its subpopulations/calculate median fluorescent intensities on FlowJo. Thus all cell subsets derived from a parent gate with below 30 events were scored as NA.

Patient grouping

Patients in this study were divided into groups using four criteria's: (1) Presence of a malignancy (cancer or non-cancer); (2) Type of cancer (solid or haem); (3) COVID-19 infection (positive or negative); and (4) COVID-19 status (active infection or recovered). Based on this criteria, we have nine separate cohorts that were used for the analysis in this study: (1) Solid cancer COVID-19⁺ active n=11; (2) Haem cancer COVID-19⁺ active n=13; (3) Non-cancer COVID-19⁺ active n=52; (4) Solid cancer COVID-19⁺ recovered n=12; (5) Haem cancer COVID-19⁺ recovered n=5; (6) Non-cancer COVID-19⁺ recovered n=22. (7); Solid cancer non-COVID-19 n=27; (8) Haem cancer non-COVID-19 n=8; (9) Healthy (non-cancer / non-COVID-19) n=46.

QUANTIFICATION AND STATISTICAL ANALYSIS

Statistical analysis details are reported in the figure legends and statistical significance are reported in the figures, highlighted in red.

Clinical data correlation and multivariate regression analysis

We used the automated Saddle Point Signature pipeline (version 2.9.3) to compute pairwise Pearson correlations between clinical covariates and COVID-19 severity (shown in a heatmap), and to identify the optimal covariates for multivariate outcome prediction, using repeated nested iterations of a Bayesian proportional hazards model with adaptive parameter priors, backward covariate reduction (using a probabilistic criterion), bootstrapping and cross-validations. The pipeline generates the optimal covariate set together with the relevant associations and risk scores, and estimators of outcome prediction performance of the optimal model on training and test data.

High dimensional data analysis of flow cytometry data

All statistical analysis was performed using R version 4.0.0. The effects of cancer and COVID-19 on each measured immune parameter were analysed by multiple regression with *sex*, *age*, *cancer status* (cancer or non-cancer), *COVID-19 status* (COVID-19⁺ or COVID-19⁻) and the interaction of *cancer status* and *covid status* as predictors. Immune parameters that were available for less than three patients in at least one cohort were excluded from the analysis. A linear regression model was fit to log-transformed blood counts, a tobit regression model (*tobit* function in the AER package, version 1.2.9) was fit to log-transformed cytokine concentrations to account for left-censoring at the limit of detection (Uh et al., 2008), and a beta regression model (*betareg* function in the betareg package, version 3.1.3) was fit to the proportion data from serology and frequency measurements.

All tests were performed on a log scale. Log fold changes were obtained as contrasts of estimated marginal means (*emmeans* package, version 1.4.8), controlled for sex and age, at the levels of *covid-19 status* and *cancer status* corresponding to the cohorts of interest (Cancer COVID-19 vs Cancer and Cancer COVID-19 vs COVID-19) and tested for statistical significance by t test (blood counts and cytokines) or Wald test (frequencies and serology) using robust standard errors (HC1 estimator, *sandwich* package, version 2.5.1) to account for heteroscedasticity between cohorts. The estimated marginal means on the log scale were obtained either directly from the model coefficients (for models fit to log-transformed data) or by log-transformation of the estimated marginal means on the measurement scale (for models fit to untransformed data). Fold changes were obtained by back-transformation.

The interaction between cancer and COVID-19 was calculated, on a log scale, as

$$\left(\log \hat{\mu}_{\text{Cancer COVID}} - \log \hat{\mu}_{\text{Healthy}} \right) - \left[\left(\log \hat{\mu}_{\text{Cancer}} - \log \hat{\mu}_{\text{Healthy}} \right) + \left(\log \hat{\mu}_{\text{COVID}} - \log \hat{\mu}_{\text{Healthy}} \right) \right]$$

where $\hat{\mu}_{\text{Cohort}}$ is the estimated marginal mean for Cohort on the measurement scale. After back-transformation, this quantity corresponds to the ratio between the observed fold change in Cancer COVID-19 vs Healthy and the fold change that would be observed in Cancer COVID-19 vs Healthy if the effect of cancer and the effect of COVID-19 were purely multiplicative.

The analysis was performed separately for solid cancer patients with active COVID-19, solid cancer patients recovered from COVID-19, haem cancer patients with active COVID-19 and haem cancer patients recovered from COVID-19. When more than one sample was available for each patient, the earliest sample with the lowest number of missing measurements was used. All p values obtained were adjusted using Storey's method (*qvalue* package, version 2.21.0) to control the false discovery rate (FDR) across all measured variables within each comparison. FDR-adjusted p values <0.05 were deemed significant.

Longitudinal blood parameters

The longitudinal plots were constructed by assigning each patient's measurements to time bins and replacing, for each patient, all the measurements in a bin with their median. Measurements at onset were tested with the Wilcoxon rank sum test, while all (paired) fold changes (peak abnormality vs pre-infection, recovery vs pre-infection and 20-29 days vs 0-3 days) were tested with the Wilcoxon signed rank test.

Correlations with severity

Kendall's τ for the semi-partial correlations of immune parameters with severity, with each immune parameter adjusted for age and sex, were calculated as described in *spcor* function of the *ppcor* package, version 1.1 (Kim, 2015). Lines on the correlation plots are constrained splines (monotonic increasing if $\rho > 0$, monotonic decreasing if $\rho < 0$).

Principal component analysis

Principal component analysis (*prcomp* function in base R) was performed separately for active and recovered patients on a log transformed, scaled and centered matrix of all measurements except serology. A subset of samples and measurements with no missing cases was selected in three steps: first, samples with more than a threshold number of missing measurements were discarded; for the remaining samples, measurements that were missing more than a threshold number of samples were discarded; finally, all remaining samples with missing cases were discarded. The thresholds were chosen to maximise the product of number of samples and number of measurements.